DOKUZ EYLÜL UNIVERSITY
GRADUATE SCHOOL OF NATURAL AND APPLIED SCIENCES

INVESTIGATION OF OPTICAL PROPERTIES AND SENSING POTENTIALS OF SOME ORGANIC DYES IN POLYMERIC MATRICES

by
Çağla KABAKCI

October, 2018
İZMİR

INVESTIGATION OF OPTICAL PROPERTIES AND SENSING POTENTIALS OF SOME ORGANIC DYES IN POLYMERIC MATRICES

A Thesis Submitted to the
Graduate School of Natural and Applied Sciences of Dokuz Eylül University
In Partial Fulfillment of the Requirements for the Degree of Master of Science
in Chemistry Program

by

Çağla KABAKCI

October, 2018
İZMİR

M.Sc THESIS EXAMINATION RESULT FORM

We have read the thesis entitled **"INVESTIGATION OF OPTICAL PROPERTIES AND SENSING POTENTIALS OF SOME ORGANIC DYES IN POLYMERIC MATRICES"** completed by **ÇAĞLA KABAKCI** under supervision of **PROF. DR. KADRİYE ERTEKİN** and we certify that in our opinion it is fully adequate, in scope and in quality, as a thesis for the degree of Master of science in chemistry.

Prof. Dr. KADRİYE ERTEKİN

Supervisor

Prof. Dr. Özlem Üstar

JuryMember

Doç. Dr. Nüket TİRTOM

JuryMember

Prof. Dr. Kadriye ERTEKİN

Director

Graduate School of Natural and Applied Sciences

ACKNOWLEDGMENTS

First of all, I would like to thank my supervisor Prof. Dr. Kadriye ERTEKİN for giving me the opportunity to carry out this work and for her valuable suggestions, encouragement and supervision.

I would like to thank to my parents and especially to my mother Gülsüm KABAKCI, my father Zeynel KABAKCI, and my brother Çağatay KABAKCI for their great supports. Without their never-ending support and encouragement, I would not be where I find myself today.

I would also like to thank my housemates Aylin FALAY and Aslı TEKBIYIK for their endless morale and support.

Finally, I thank all my friends, specialists and professors at EMUM and faculty of science for all of the invaluable help, friendship and encouragement.

Çağla KABAKCI

INVESTIGATION OF OPTICAL PROPERTIES AND SENSING POTENTIALS OF SOME ORGANIC DYES IN POLYMERIC MATRICES

ABSTRACT

In this thesis, spectral properties and selective sub-nano molar response towards the ionic silver of the newly synthesized Y10 dye has been investigated. The excitation and emission spectra of the dye has been recorded in the solutions of tetrahydrofurane (THF), diclorometane (DCM) and ethyl alcohol (EtOH). Herein we investigated spectral properties of the fluorescent Y10 dye in plasticized polyvinyl chloride (PVC) polymethyl methacrylate (PMMA) and in ethyl cellulose (EC). In addition to the plasticizer the lipophilic anionic additive and ionic liquid were also utilized and effect of these additives on the spectral response has been evaluated. The Y10 dye exhibited better spectral response in EC. In later studies the EC has been used as matrix material.

Response towards the ionic silver has been investigated in phosphate buffered solutions at pH 7.06 for the IL-Free and IL-Doped composites. The best limit of detection (LOD) value has been reported as $1.1x10^{-15}$ M silver. The decay time measurements were used to explain the mechanism behind the response. While the IL-Doped films exhibiting a linear response for the concentration range of 10^{-4}-10^{-12} M, the electrospun fibers made up of the same material exhibited the linear response for the concentration range of 10^{-8}-10^{-12} M.

The EC doped Y10 dye exhibit as selective spectral response towards silver in presence of excess amounts of mercury(II), aluminum(III), calcium, copper(II), iron(III), potassium, manganese, magnesium, and lead at neutral pH. When the dye doped into EC along with appropriate additives can be used as an emission based sensor for silver for a large linear concentration range of 10^{-12} to 10^{-4} M.

Keywords: Sensor, optical chemical sensor, fluorescence, ionic liquid, Ag(I)

BAZI ORGANİK BOYALARIN POLİMERİK MATRİSLERDE OPTİK ÖZELLİKLERİ VE POTANSİYELLERİNİN İNCELENMESİ

ÖZ

Bu tezde, yeni sentezlenmiş Y10 kodlu organik boyar maddenin spektral özellikleri araştırılmış, nano-molar altı konsantrasyonlardaki gümüşe seçimli emisyon bazlı davranışı incelenmiştir. Boyanın tetrahidrofuran (THF), diklorometan (DCM) ve etil alkol (EtOH) gibi çözücülerde, absorpsiyon eksitasyon ve emisyon spektrumları kaydedilmiştir. Bu çalışmada yüksüz ve floresans özellik gösteren Y10 boyasının plastikleştirici içeren etil selüloz (EC), polivinil klorür (PVC) ve polimetil metakrilatta (PMMA) spektral özellikleri incelenmiştir. Yapılan testlerde, plastikleştiricinin yanında lipofilik anyonik katkı maddesi ve iyonik sıvı da kullanılmış ve spektral cevabı etkileri değerlendirilmiştir.Y10 boyasının diğer katı matrislere göre EC da daha iyi sonuçlar verdiği görülmüştür. Matriks malzemesi olarak EC polimeri kullanılmıştır.

Y10 boyasının EC da gümüşe olan cevabı, fosfat tamponunda (pH 7.06) iyonik sıvı içeren ve içermeyen formlar üzerinden iki farklı aşamada araştırılmıştır. En iyi tayin limiti $1.1x10^{-15}$ M gümüş olarak belirlenmiştir. Mekanizmaların aydınlatılmasında "floresans ömrü" ölçümleri kullanılmıştır. İyonik sıvı içeren ince filmler 10^{-4}-10^{-12} M aralığında lineer cevap verirken aynı malzemeden hazırlanmış fiberler 10^{-8}-10^{-12} M aralığında cevap vermiştir.

Y10 boyası EC matrise doplandığında, nötral pH da civa(II), alüminyum(III), kalsiyum, bakır(II), demir(III), potasyum, mangan, magnezyum ve kurşun(II) nin yanında gümüşe seçimli olarak cevap vermiştir. Boyanın uygun katkı maddeleri ile birlikte kullanıldığında 10^{-12} ile 10^{-4} M arasında değişen geniş konsantrasyon aralığında gümüş iyonlarına emisyon bazlı lineer cevap verdiği ortaya konmuştur.

Anahtar Sözcükler: Sensör, optik kimyasal sensör, floresans, iyonik sıvı, Ag(I)

CONTENTS

Page

LIST OF FIGURES

Page

LIST OF TABLES

Page

CHAPTER ONE
INTRODUCTION

1.1 Chemical Sensors

A chemical sensor is generally a small device that gives a signal arising from a chemical reaction or a process taking place between the analyte and the sensor device. Such a sensor can be used for the qualitative or quantitative analysis of the analyte of interest (Zeyrek Ongun, 2013).

According to the“Cambridge definition”: a chemical sensor is a miniaturised device that can deliver real time and on-line information on the presence of specific compounds or ions in even complex samples (McDonagh, Burke, & MacCraith, 2008).

Applications of chemical sensors can be listed as cation and anion recognition, process and quality control, critical care unit monitoring devices, homeland security, safety, industrial hygiene and engineering controls, recognition of air pollutants, diagnosis of biomarkers and blood gases (Stetter, Penrose, & Yao, 2003).

1.1.1 Optical Chemical Sensors

Optical chemical sensors or optods are a class of chemical sensors. They are compact, practical and suited to miniaturization. They are resistant to electrical interference and has the advantage of sensitivity of spectrophotometric measurements. Most of the optical chemical sensors use chromophor molecules along with appropriate additives immobilized in polymeric forms. (Ensafi&Bakhshi, 2003)

According to the International Union of Pure and Applied Chemistry (IUPAC) a chemical sensor is;

“A device, that transforms chemical information, ranges from the concentration of a specific sample component to total composition analysis, into an analytically useful signal. The chemical information, mentioned above, may originate from a chemical reaction of the analyte or from a physical property of the system investigated. Chemical sensors contain two basic functional units: a receptor and a transducer part (Figure 1.1).Some sensors may include a separator which is, for example a membrane (IUPAC, 1997)” (EPA, 2012).

Optical sensors are mainly based on different optical principles like absorbance, reflectance, scattering, refractive index, polarization, fluorescence or phosphorescence. They may use different regions of the electromagnetic spectrum; ultraviolet, Visible, Infrared, or Near infrared (Jerónimo, Araujo, & Montenegro, 2007).

Optical chemical sensors exhibit a number of advantages over conventional electrochemical sensors, in terms of selectivity, interference, and safety. They do not require reference cell like potentiometric devices. Additionally, they are sensitive, inexpensive, non-destructive, robust and are miniaturazible. They are also called as optrodes. This word can be considered as a combination of the words of optode and electrode. Furthermore, they allow multiple analyses with a single device (Lukowiak & Strek, 2009).

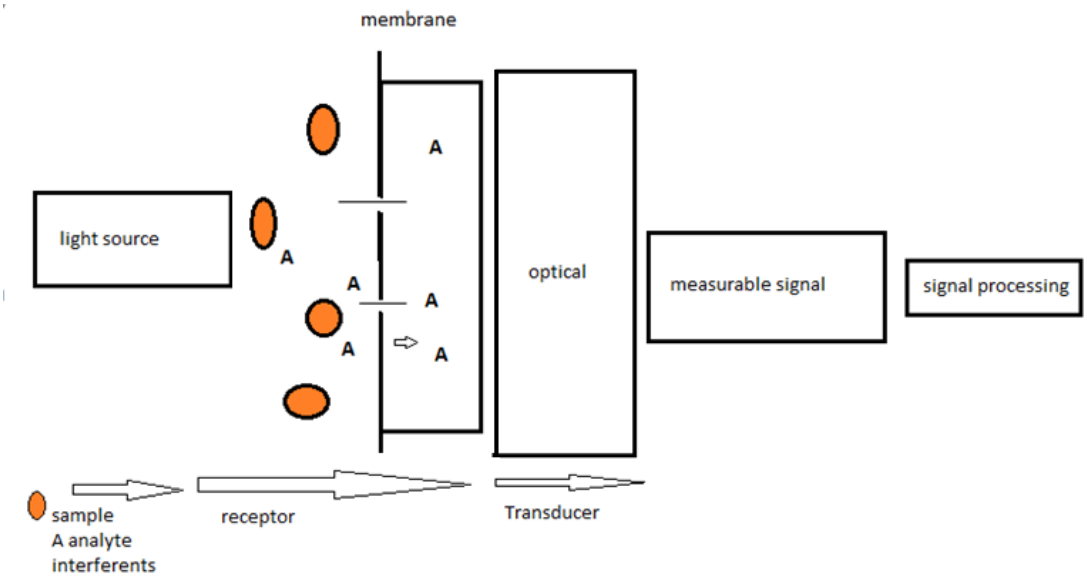

Figure 1.1 Schematic representation of an optical chemical sensor

Optical chemical sensors mainly use the components of spectroscopic devices but in a miniaturized form. These are light sources of, lasers or LEDs (Light Emitting Diodes), detectors of photo diodes or sometimes photo multiplier tubes, and auxillary components of fiber optics, amplifiers and others. If the analytical signal arises from variation of either absorption or emission, the intensity and/or wavelength of the light may be followed as the analytical signal. Sometimes other optical properties including diffraction, refractive index, reflection etc. may be used as the analytical signal (Mayr, 2002).

1.1.1.1 Classification of Optical Chemical Sensors

Optical sensors can be classified in many different ways. If the fiber optics were utilized in the structure of the sensor, they called as fiber optic chemical sensors. They also can be classified according to the analyte. In such a classication the sensors can be named as "cation or anion sensors, pH sensors, gas sensors O_2, CO_2 etc", or "biosensors" (Zeyrek Ongun, 2013).

Chemical sensors may be classified according to the operating principle of the transducer (Table 1.1).

Tablo 1.1 Classification according to the operating principle of the transducer

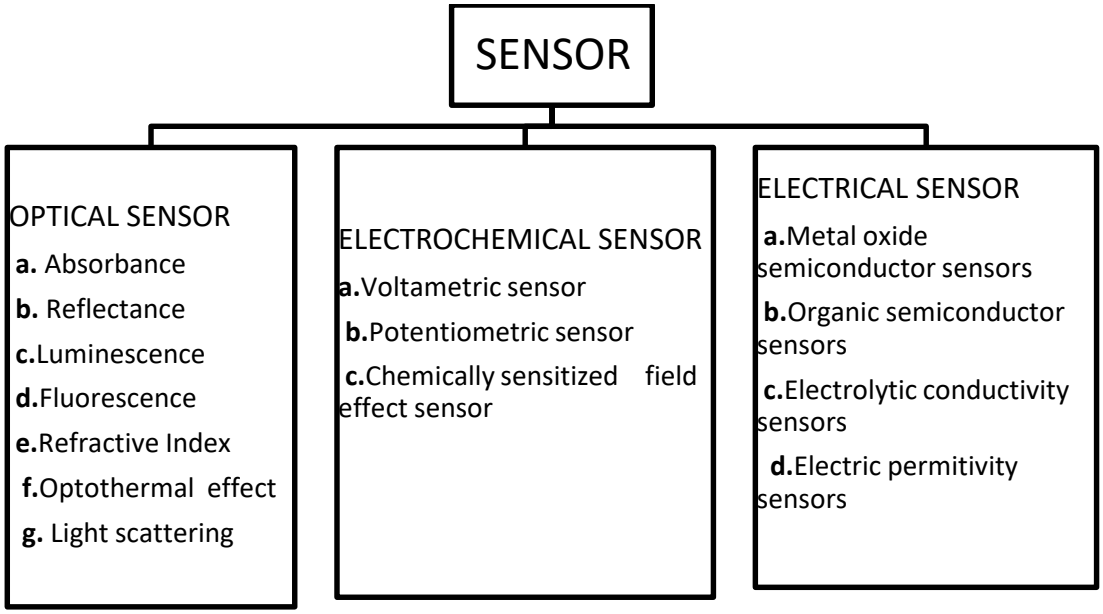

In such designs probably the most intensively measured optical properties are absorption, fluorescence intensity, and decay time. However, measurement of the scattering, reflectance, refractive index, and polarization is also possible as the analytical parameter (Wencel, Abel, & McDonagh, 2014). Absorbance arising from the chromophore or chromoionophore should be measured in a transparent medium. The measurement can be performed both in solution phase and in solid state.

Luminescence, is the emission of the light after an excitation process and can be classified as fluorescence and phosphorescence. Luminescence takes places upon excitation of the chromophore or the chromoionophore. The emission based data may be acquired both from the solution phase and the solid state. Variations in reflectance and refractive index, light scattering by a particle or a surface in a solution or in vacuum may also be recorded as the analytical signal.

1.1.1.1.1 Optical pH Sensors. Optical pH sensors mainly uses pH sensitive dyes in an immobilized form in a polymeric matrix together with additivies. The indicator dyes are typically weak organic acids or bases with chromophore properties. Their protonated (acidic) and deprotonated (basic) forms exhibit different colors, absorption and/or emission characteristics. In most of the optical pH sensors the pH sensitive indicator, immobilized in a proton-permeable solid matrix, which reversibly works upon protonation. Since the highest sensitivity is observed at pH close to the pKa, the pH indicators should be chosen considering their pKa value. The indicator dyes change their spectral properties, such as absorption, fluorescence, or reflectance, as a function of the pH of the environment (Wencel, Abel, & McDonagh, 2014).Up to now fluorescein and derivatives 1,9,14 (Tian, et all., 2013; Lobnik, Oehme, Murkovic, & Wolfbeis, 1998; Weidgans, Krause, Klimant, & Wolfbeis, 2004). porphyrins and Hydroxy-3,6,8-pyrenetrisulfonate (HPTS), (Schulman, et all., 1995; Kermis, Kostov, & Rao, 2003). have been used many times as indicators in the design of the solid-state pH sensors. On the other hand, polyvinyl chloride (PVC), ethyl cellulose (EC), polymethyl methacrylate (PMMA) and sol-gel based materials have been used as support materials in the design of optical chemical pH sensors.

1.1.1.1.2 Sensors for Gases. CO2, O2 and toxic gases such as NH3, H2S, Cl2, SO2, HCHO, HCl, etc. can also be measured by optical chemical sensing approach. The indicator chemistry can be combined with optical fibres to produce devices. In these designes not only the indicator but also the matrix material should be selective for the analyte. In the optical sensing of oxygen, silicon and sol-gel based matrices are appropriate. In case of CO2 ethyl cellulose may be more advantageous (Oter, 2007).

1.1.1.1.3 Optical Cation Sensors. Recent years, chemical sensors for heavy metal ions have been focus of interest. Such kind of sensors can be described as devices which are capable of responding to the presence of one or more metal ion or heavy metal ion in a reversible manner. In such kind of sensors the optical properties may be measured by absorbance, fluorescence and/or reflectance spectroscopy or with miniaturized devices. Sometimes the sensors may be prepared in various forms such as practical test strips, capillary devices, microfluding systems or using optical fibres and integrated optics (Oehme &Wolfbeis, 1997).

Today the field of cation sensing is well understood and a large number of sensors for metal cations, particularly for ions such as Na^{+} (Englich, et al., 2011). K^{+} (Ertekin, Tepe, Yenigül, Akkaya, & Henden 2002). Mg^{2+} and Ca^{2+} (Saleh, Elkady, Ali, Alminderej, & Mohamed, 2018). and other heavy metal ions have been developed (Kaçmaz, et all., 2011; Topal, et all., 2010; Zhao, et all., 2017) (Venturini, Baumgartner, & Borisov, 2018) (Borgohain, Boruah, Baruah, 2016) (Dey, Sarkar, Maity, & Roy, 2017).

1.1.1.1.4 Optical Anion Sensors. Anions are quite important and abundant in nature and in biological processes. Among them the analysis of the conventional anions of Cl^{-}, I^{-} (Nugent, H. Lee, Reibenspies, H.S Lee, & Hancock, 2017) NO_2^{-}, NO_3^{-}, PO_4^{3-}, SO_4^{2-} and HCO_3^{-}(Aydoğdu, Ertekin, Göçmentürk, Ergün, & Çelik, 2014) is very important. Sometimes presence of the anions is releated to the industrial and agricultural proceses. CN^{-} (Yanar, et all., 2016) and arsenate are the toxic anions and arises from industrial proceses. Therefore, development of practical,

sensitive and selective optical sensors for their easy detection of these specials is quite important. Especially fluorescent sensors are effective tools for recognition of anions due to their high sensitivity even for low analyte concentrations (Veale, & Gunnlaugsson, 2010).

1.2 Polymers for Optical Sensors

1.2.1 Role of Polymeric Matrix Materials in Optical Sensors

Polymers are frequently used as matrix materials to encapsulate and protect indicator dye from the potential interferents in optical sensor design. By this way the indicator has been immobilized in form of thin film or to the tip of an optical waveguide or an optical fiber which is then brought into contact with the analyte solution (Baldini et al., 2006).

Used polymeric matrix materials in the sensor design are expected to satisfy different requirements. The encapsulated dye and all other additives have to be soluble and stable within the polymeric matrix without leaching. The analyte should be diffusible into the polymer. The chosen polymeric matrix material has to be selective towards to analyte and chemically and physically stable to provide long lifetime and stability requirements.

Swelling, migration or reorientation of the indicator dye as well as the other additives, crack formation and crystallization are not desirable within the polymeric matrix. Other desired properties of the polymeric matrix materials are to be resistant to heat, light, acids, bases, oxidizing agents and being environmentally friendly and if it is possible it should be biocompatible. The matrix material preferably should not exhibit any intrinsic color/luminescence, and if it is possible it should be optically transparent in the studied spectral range (Mohr, 2002)

1.2.2 Polymers Used in Optical Chemical Sensor Design

1.2.2.1 Hydrophobic Polymers

Such kind of polymers are not soluble in water. Poly (vinyl chloride) (PVC) poly (methyl methacrylate) (PMMA), polystyrene and poly (vinyl acetate) (PVA) are the typical examples of the hydrophobic polymers (Table 1.2). In order to provide flexibility and diffusebility the plasticizers may be added into the matrix containing the hydrophobic polymers. By the addition of the plasticizers, polarity, lipophilicity, selectivity and sensitivity of the polymer can be tuned. Only the neutral indicator dyes can be immobilized into the hydrophobic polimers by encapsulation (Mohr, 2002). The positively or negatively charged dyes will be rejected by the polymers. However, some modifications may allow the immobilization of such kind of charged dyes to the surface of the polymeric matrices.

Table 1.2 Chemical structures of hydrophobic polymers (Personal.uni-jena, 2012)

POLYMER	POLYMER NAME
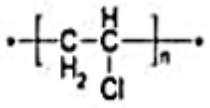	**Poly(vinyl chloride)** (PVC)
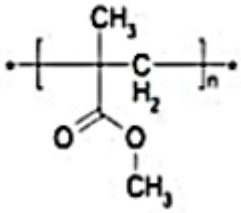	**Poly(methyl methacrylate**) (PMMA)

Table 1.2 continues

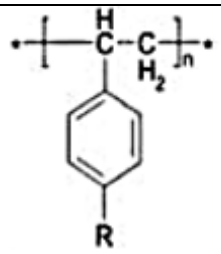	**Polystyrene** (PS)
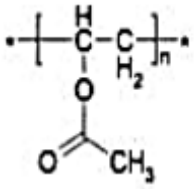	**Poly(vinyl) acetate** (PVA)

1.2.2.2 Hydrophilic Polymers

The hydrophilic polymers may contain hydrogen-bonding functional groups such as hydroxyl, amino, or carboxamide. Typical examples of the hydrophilic polymers can be listed as proteins (wool, cotton, silk etc.) cellulose and derivatives, polyethylene, polyamides, polyacrylic amides, polyurethanes, polyacrylates, polyglycols, and variety of hydro gels (Lobnik, Turel, & Urek, 2012) (Table 1.3).

Hydrophilic polymers are competable to an aqueous environment. Ion diffusion is easy, but the potential water uptake (1-100 %) may cause swelling of the polymer. This issue affects optical properties of the sensors which is not desirable (Baldini et al., 2006).

Table 1.3 Hydrophilic polymers (Personal.uni-jena, 2012)

POLYMER	POLYMER NAME
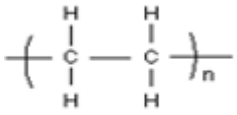	**Polyethylene** (PE)
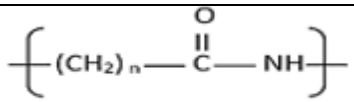	**Polyamides** (PA)
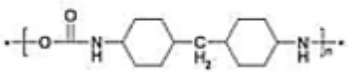	**Polyurethane** (PU)
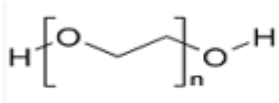	**Polyglycol**
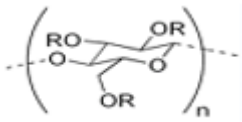 R=CH_2CH_3	**Ethyl cellulose** (EC)

1.2.2.3 Non-polar Polymers

Polymers can also be classified as ‘polar’ or ‘non-polar’ considering their behavior under electric field or under voltage. In case of polar polymers, dipoles are created in the presence of an electric field. This will create ‘dipole polarization’ of the polymers like PMMA, PVC, PA (Nylon), PC.

The non-polar polymers are generally symmetrical and there are no dipoles in their structure. Examples of non-polar polymers are Poly(dimethyl siloxane),

polytetrafluoroethene (PTFE) and many other fluoropolymers, PE, PP and PS (Table 1.4). These materials tend to have high resistivities and low dielectric constants. They are appropriate matrix materials for molecules without electrical dipole but not appropriate for polar species, ionophores, cationic or anionic forms of the sensor dyes and the analytes (Mohr, 2002).

Table 1.4 Nonpolar polymers (Personal.uni-jena, 2012)

POLYMER	POLYMER NAME
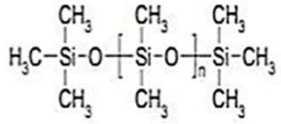	**Poly(dimethyl siloxane)**
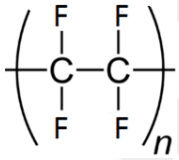	**Polytetrafluoroethene** (PTFE)
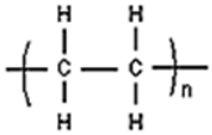	**Polyethylene** (PE)
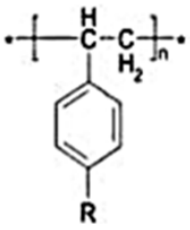	**Polystiren** (PS)

1.2.2.4 Ionic Polymers (Polyelectrolytes)

This kind of poymers (Table 1.5) bear a large amount charged groups on their structure. Generally, the anionic polymers are appropriate for binding of cationic dyes. Conversly the anionic dyes can easily be immobilized on to the oppositely charged polymers. They can also be used to exchange their counter ions with

indicator ions. Trimethylammonium methyl cellulose and polyaniline are examples of cationic polymers. Nafion and polystyrene sulfonates are the anionic forms (Baldini et al., 2006).

Table 1.5 Ionic polymers (Personal.uni-jena, 2012)

POLYMER	POLYMER NAME
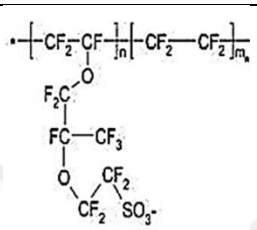	**Nafion (anionic polymer)**
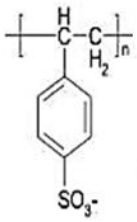	**Polystyrene sulfonates (anionic polymer)**
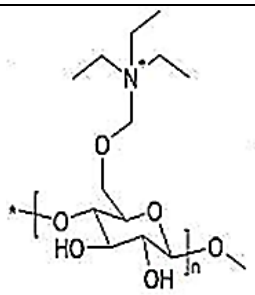	**Triethylammonium methylcellulose (cationic polymer)**
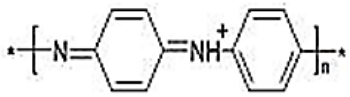	**Polyaniline (cationic polymer)**

1.3 Optical Parameters Measured Working with Optical Chemical Sensors

In most of the optical chemical sensors, absorption, fluorescence or phosphorescence intensity or the fluorescence lifetime has been measured as the analytical signal. However, the parameters of refractive index, reflectance and light

scattering can also be measured. In this thesis mainly fluorescence based measurements were performed. The spectral data was also supported by the absorption and decay time measurements. Therefore, a short explanation of the absorption and luminescence is given below.

Reflectance is the fraction of the total radiation incident upon a surface and varies with the wavelength distribution of the incident radiation.

Refractive index has been explain as the ratio of the rapidity of light in vacuum to that in a given medium and measured after all a change in solution composition.

Light scattering, light in the form of spreading energy is diffused by a particle in solution or in vacuum.

Luminescence can shortly be defined as the intensity of light emitted after an excitation process. The two well-know types of luminescence are fluorescence and phosphorescence.

Fluorescence is the intrinsic property of some molecules or atoms. Some type of molecules or atoms absorbs the light at a particular wavelength and generally emits the light at a longer wavelength. or simply fluorescence is generally referred to as the emission of photons following the absorption of the light. Luminescence may be classified as chemiluminescence, thermoluminescence, catodoluminescence photoluminescence and triboluminescence according to the source of the excitation. Fluorescence may be measured for both transparent and opaque moieties.

1.3.1 Luminescence

1.3.1.1 Theory of the Luminescence

Luminescence is a chain of sophisticated events but simply is light emission from the electronically excited atoms or molecules (Lakowicz, 1993; Parker, 1968; Schmidt, 1994).

Perrin–Jablonski diagram show us all of the possible processes consisting of luminescence. These are photon absorption, internal conversion, fluorescence, intersystem crossing, phosphorescence, delayed fluorescence and sometimes triplet–triplet transitions, respectively (Figure 1.2). Herein, the singlet electronic states referred as S_0 (ground electronic state). The excited electronic states denoted as S_1 or S_2 and triplet states as the T_1; $T_2 \ldots T_n$, respectively. Vibrational energy levels are exist for each of these electronic states. Luminescence process initiates with the excitation. Among these processes absorption is the fastest one and occurs within a very short time scale; $1x10^{-15}$ s. (Lakowicz, 1993; Parker, 1968; Schmidt, 1994).

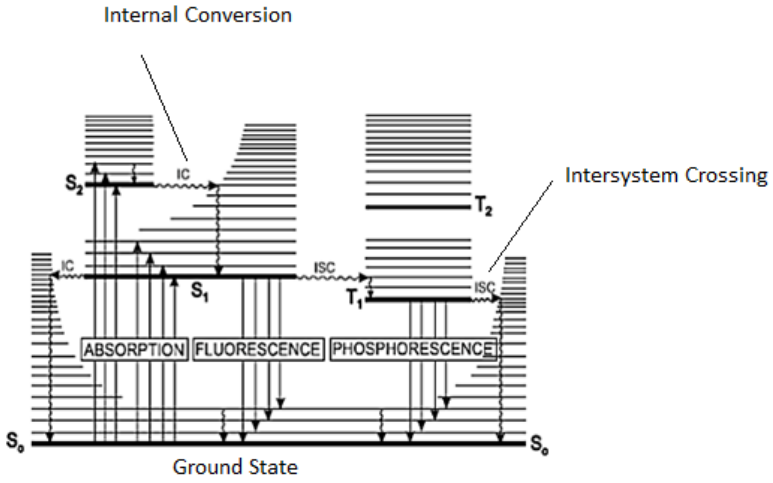

Figure 1.2 The Perrin–Jablonski diagram (Valeur, 2002)

1.3.1.1.1 Internal Conversion (IC). Internal conversion is a radiationless transition taking place between two electronic states of the same multiplicity. Herein the multiplicity is an indication of the number of possible orientations for the same

spatial electronic wavefunction in a molecule or atom. The IC is sometimes called “radiationless deactivation”, because no photons are emitted. The energy of the electronically excited state is given off to vibrational levels of the atom or molecule or sometimes to the solvent or close proximitiy of the emitting species which is generally converted into heat (Valeur, 2002).

1.3.1.1.2 Fluorescence. Some molecules and/or atoms absorb light at a certain wavelength and the electrons move from the ground state (S_0) to one of the excited states (S_1) or (S_2) or further levels. Emission of photons from the lowest vibrational level of the S_1 to S_0 by relaxation is called ‘fluorescence’. The emitted light generally appears at a longer wavelength after a very short time interval, which is approximately between the 10^{-9}-10^{-7} seconds. Figure 1.3 reveals basic pathways of fluorescence.

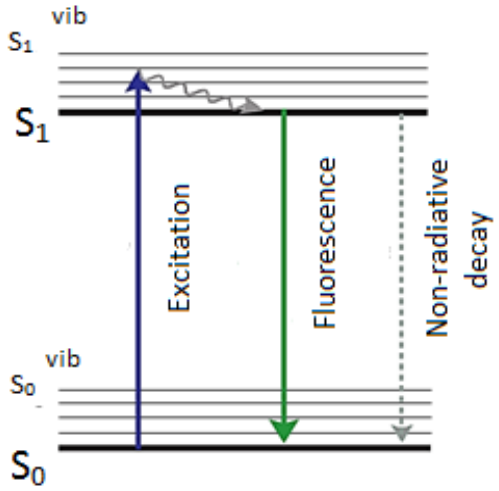

Figure 1.3 Basic transitions taking place during fluorescence

1.3.1.1.3 Intersystem Crossing (ISC). Intersystem crossing is a non-radiative process in which a singlet excited electronic state makes a transition to a triplet excited state belonging to different multiplicities (Valeur, 2002). According to IUPAC definition ISC is a photophysical process. An isoenergetic radiationless transition between two electronic states having different multiplicities occurs

Intersystem crossing may take place in the time interval of 10^{-7}–10^{-9} seconds unless competing with other pathways of fluorescence.

1.3.1.1.4 Phosphorescence. During phosphorescence, excited molecules undergo a transition to a lower lying metastable state that can last for longer time with respect to the fluorescenc. In case of phosphorescence, the excited electron undergoes an intersystem crossing which is generally a triplet state. The energy trapped in the triplet state is generally return to the lower energy levels with only "forbidden" transitions which are kinetically unfavored and occur at slower time intervals with respect to the fluorescence. Most phosphorescent compounds exhibit lifetimes on the order of milliseconds. Rarely, some phosphors and/or afterglow phosphors may exhibit triplet lifetimes extending to minutes or even hours. Figure 1.4 reveals basic pathways of phosphorescence.

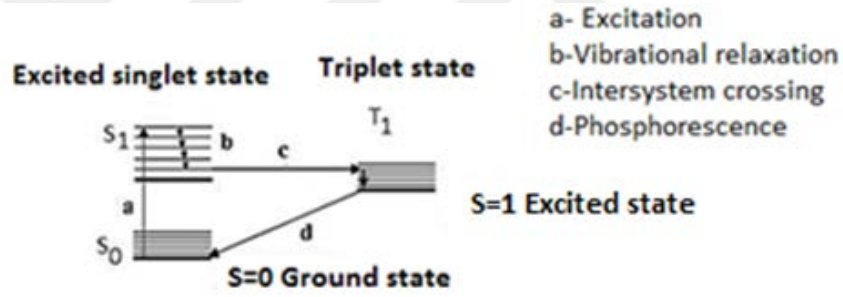

Figure 1.4 Basic transition taking place during phosphorescence

1.3.1.1.5 Stoke's Shift. Stokes shift can be defined as the difference between the peak maximum of the absorption and emission spectrum of the related molecule. Because the energy of the absorption is typically higher than the fluorescence emission, wawelength of the resulting emission maxmium appears at longer wavelengths with respect to the absoption maximum. The schematic diagram of Stoke's shift has been shown in Figure 1.5.

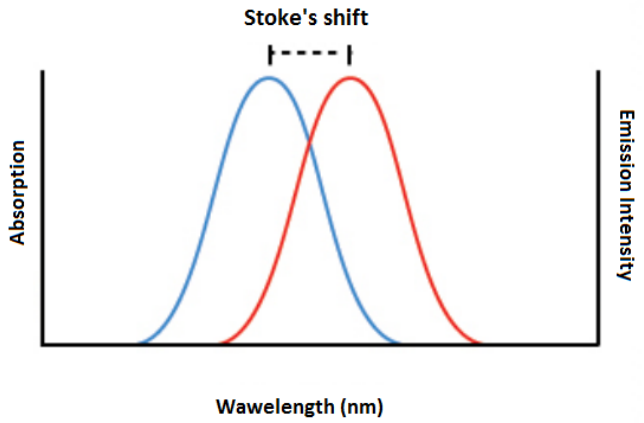

Figure 1.5 Schematic representation of the Stoke's shift

1.3.1.2 Factors Effecting Fluorescence

Some factors affect the fluorescence dynamics. The most important factors effective on the fluorescence are; solvent polarity, concentrations of species, pH and micro-environment of the molecule

Fluorescence spectrum of a molecule is strongly dependent on its micro-environment. This effect becomes extremely important in solution phase and in case of fluorophores with large excited-state dipole moments. This kind of fluorophores exhibit spectral shifts in emission spectrum to longer wavelengths when they dissolved in polar solvents (Fluorescence fundamentals, 2015).

When studying at high concentrations, it is strongly possible that quenching of one fluorophore by another. Therefore, studying in diluted solution ($< 10^{-5}$ M) is necessary to prevent the self-quenching. Some of the fluorophores have proton bonding (sensitive) centers on their structure. In such cases fluorescence becomes pH dependent.

1.3.1.3 Fluorescence Lifetime

The "fluorescence lifetime" is the average time for a molecule to remain in the excited state (Lakowicz, 1993). Fluorescence lifetimes are generally on the order of

1-10 nanoseconds. However, they can range from hundreds of nanoseconds to the sub nanosecond time-scale. The lifetime of fluorescence is the characteristic property of the excited singlet state. The excited states generally decay exponentially by time and can be formulated by following equation;

$I = I_0 e^{-t/\tau}$

where I_0 is the initial intensity, I is the intensity after some time later, t is the time and τ is the lifetime of the excited state. $kF = 1/t$, where k is the rate constant of fluorescence.

In another way, the decay time can be defined as the time for the intensity to drop by 1/e or to 37% of the τ.

Figure 1.6 shows a typical decay curve. The lifetime equation can also be written in terms of rate constants (k_r–radiative rate, k_{nr}- non radiative rate) as well as in terms of the fluorescence quantum yield (φ).

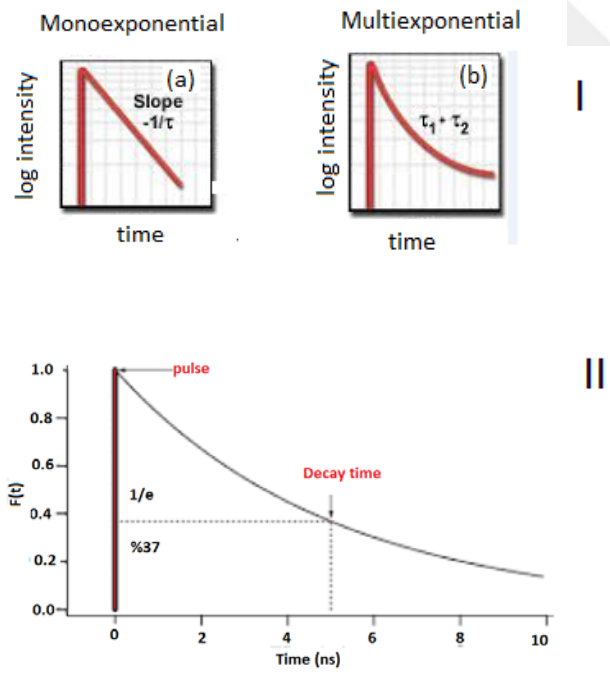

Figure 1.6 Fluorescence lifetime decay profiles I: monoexponential and multiexponential decay profiles II: decay time

The decay law may follow first order kinetics; sometimes fluorescence decays may be more complex and may fit multi- exponential decays. If the excited molecules are in inhomogeneous micro environments multi- or non-exponential decays may be observed. Plots of single and multi-exponential decays are shown in Figure 1.6.

The fluorescence lifetime is an intrinsic property of a molecule and is independent of the sample concentration. The fluorescence lifetime is also independent from the fluctuations in the light source arising from voltage or photo bleaching which is an advantage of the lifetime measurements over steady-state ones.

Fluorescence lifetimes can be measured by two different approaches; the time domain and frequency domain.

In the time domain mode, excitation should be performed by a pulsed light source and fluorescence of the sample is recorded as a function of time. Depending on the required sensitivity, the time resolution can be performed by different ways: Time Correlated Single Photon Counting technique (TCSPC), streak camera and intensified CCD cameras can be used for the measurement of time resolution.

1.3.1.3.1 Frequency Domain Lifetime Measurement. In case of frequency-domain measurements, the excitation is performed by a modulated light source. Because of the time difference between the absorption and emission, a phase shift occurs between these two waves and the emission is delayed in time relative to the excitation. The delay is measured in terms of phase shift and the decay time can easily be calculated from the phase shift (Lakowicz, 1993; Parker, 1968; Schmidt, 1994).

CHAPTER TWO
2. EXPERIMENTAL METHOD AND INSTRUMENTATION

2.1 Reagents

In this thesis, the polymers polymethyl methacrylate (PMMA), ethyl cellulose (EC) were used as support materials and were purchased from Across and Sigma-Aldrich, respectively. The plasticizer, dioctyl phthalate (DOP) and lipophilic anionic additive; potassium tetrakis-(chlorophenyl) borate (PTCPB) and room temperature ionic liquid (1-Butyl-3-methylimidazolium tetrafluoroborate), were supplied from Sigma-Aldrich. Tetrahydrofurane (THF) was of analytical grade and purchased from Merck. Solvents for the spectroscopic studies were used without further purification.

Buffer components; acetic acid/acetate, phosphate and metal salts were of reagent grade and were provided from Merck and Fluka. Aqueous solutions were prepared by freshly deionized ultra pure water with a specific resistance of >18.2 M Ωcm and pH 5.5. The deionized water was prepared by a Millipore reagent grade water system.

2.2 Preparation of the Buffer Solutions

2.2.1 Preparation of 0.005 M H_3PO_4 Buffer

0.057 mL (d=1.71 and 14.83 Molar) phosphoric acid was added into 150 mL ultra pure water. The solution was titrated to desired pH at 20 ^oC either with 0.1 M HNO_3 or 0.1 M NaOH. The resulting solution was completed to 200 mL with ultra pure water in a volumetric flask. The buffer solutions in the range of pH 2.0-3.0, were prepared by this way by adjusting to the desired pH.

2.2.2 Preparation of 0.005 M Acetic Acid / Acetate Buffer

0.143 mL of acetic acid (d=1.05 and 17.48 Molar) was dissolved in 450 mL ultra pure water. The solution was titrated to pH 5.0 at 20 ^{o}C either with 0.1 M HNO_3 or 0.1 M NaOH as needed. The resulting solution was completed to 500 mL with ultra pure water in a volumetric flask. The buffer solutions in the range of pH 4.0-7.0 were prepared by this way by adjusting to the desired pH.

2.2.3 Preparation of 0.005 M NaH_2PO_4 / Na_2HPO_4 Buffer

0.78 g of $NaH_2PO_4.2H_20$ (MA=156.01) and 1.79 g of $Na_2HPO_4.12H_20$ (MA=358.14) were dissolved in 950 mL ultra pure water. The solution was titrated to pH 7.0 at the lab temperature of 20 ^{o}C either with 0.1 M HNO_3 or 0.1 M NaOH as needed. The resulting solution was made up to 1000 ml with ultra pure water in a volumetric flask. The buffer solutions in the range of pH 7.0-9.0 and 10-12 were prepared by the same way by adjusting to the desired pH.

2.3 Structural Specification of the Exploited Ionophore

Herein we used the Y10 dye for the first time in the EC matrix along with ionic liguid for the sensing of ionic silver. In our previous studies we tested the Y10 dye in the polyvinylchloride (PVC) matrix for mercury and bicarbonate sensing purposes in acetic acid/acetate buffered solutions at pH 4.0 (Zeyrek, 2008). The dye exhibited quenching based response towards Hg(I) ions. However, in phosphate buffered solutions at neutral pH the Y10 dye exhibited a selective response towards Ag ions.

The silver sensitive fluorescent ionophore, 1, 4- henylenebis (azaneylylidene)) bis (methaneylylidene))bis(N,N-dimethylaniline (Y10) (Figure 2.1) was synthesized in our laboratories by Professor Y. ERGUN according to the literature method and characterized with ^{1}H NMR and IR based data (Sinha, Jain, Tilekar, Upadhayaya, Kishore, Jana, & Arora, 2005).

IR (KBr) ν: 2913 cm^{-1} (aliphatic CH), 1615 cm^{-1} (C=C), 1597 cm^{-1} (C=N), 1364 cm^{-1} (C-N).

^{1}H NMR ($CDCl_3$, 400MHz δ(ppm)): 3.06 (s, 12H, N-CH_3), 6.65 (dd, 4H, ArH, J=8.0Hz, J=1,2 Hz), 6.81 (m, 4H, ArH), 7.50 (m, 4H, ArH), 8.66 (S, 2H, N=CH).

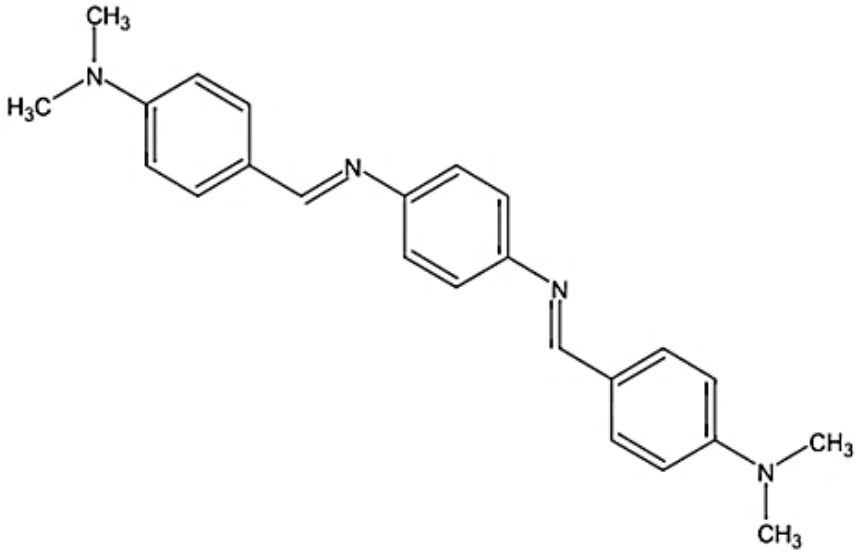

Figure 2.1 Structure of the silver sensitive fluoroionophore, Y10

2.4 Preparation of Electrospun Nano-Fibers and Thin Films

The sensing composites were prepared by mixing 120 mg of polymer (EC) or PMMA, 240 mg of plasticizer (Dioctyl phthalate, DOP), 2 mg of ionophore (Y-10 dye), equivalent amount of potassium tetrakis (4-chlorophenyl) borate (PTCPB) in 2.0 mL of THF under magnetic stirring. Chemical structures of the exploited polymers, plasticizers, lipophilic anionic additive, and RTIL were shown in Table 2.1. (Ongun, Ertekin, Gocmenturk, Ergun, & Suslu, 2012).

Experimental conditions were optimized to form bead-free fibers varying concentrations of plasticizer, PTCPB, EC and RTIL (1-Butyl-3-methylimidazolium tetrafluoroborate) in the precursor polymer solution. Ionic liquid-free (IL-free) and IL-doped forms are prepared. The amount of the RTIL in the cocktail was optimized

at 48 mg RTIL/360 mg polymer. We find that the presence of the RTIL in the polymer solutions facilitates the production of fibers under electrospinning conditions. This enhancement can be attributed to the ionic conductivity of the RTIL (Uyar, Balan, Toppare, & Redenbacher, 2009)

Table 2.1 Structures of EC, DOP, PTCPB and RTIL

Chemical Structures	Name
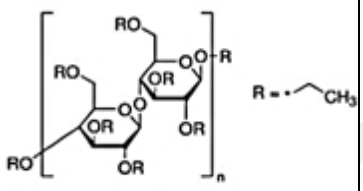	Ethyl cellulose (EC)
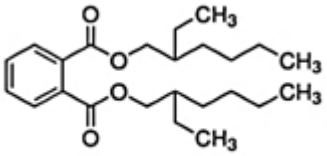	Dioctyl phtalate (DOP)
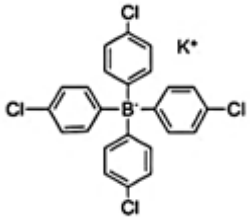	Potassium tetrakis-(chlorophenyl) borate (PTCPB)
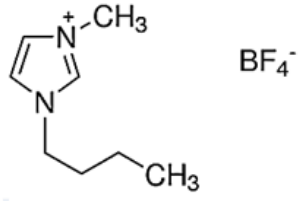	1-Butyl-3-methylimidazolium tetrafluoroborate (RTIL)

2.4.1 Fabrication of Electrospun Fibers

Electrospinning was used to fabricate EC (Ethyl cellulose) based continuous fibers.

For the fabrication of nanofibers, the polymer solution was taken in a 10 mL plastic syringe and an electric potential of 25 kV was applied between the needle and the substrate of an aluminum sheet. The distance between the needle and the electrode was adjusted to 10 cm while the diameter of the needle was 0.40 mm. The solution flow rate was maintained at 1 mL/h. When the high voltage is applied, electrically charged polymeric solution produced a spray. Meanwhile solvent evaporated and electrospun fibers were deposited on the substrate.

The fibers collected on the aluminum substrate, the mats were cut, fixed into the cuvette and the excitation or emission spectra were recorded.

2.4.2 Thin Film Fabrication

The thin films were prepared by the same composites explained for the electrospun fibres. The resulting mixtures were spread onto a 125 µm polyester support (Mylar TM type) with knife-coating and the excitation and/or emission spectra were recorded.

2.5 Apparatus and Experimental Setup

2.5.1 Spectrophotometer and Spectrofluorometer Apparatus

The absorption spectra of the dye solutions and transparent sensor films were recorded by using a Shimadzu 1801 UV-Visible spectrophotometer. Steady state fluorescence emission and excitation spectra were measured using a spectrofluorometer from Edinburgh Instruments (UK) equiped with a xenon lamp.

2.5.2 Electrospinning Apparatus

The sensing viscous PMMA or EC solutions were placed in a 10 mL plastic syringe fitted with a metallic needle of 0.4mm of inner diameter. The syringe is fixed vertically on the syringe pump (Top Syringe Pump Top-5300) and the electrode of the high voltage power supply (Gamma High Voltage ES30) was clamped to the metal needle tip. Photograph of the used electrospinning apparatus has been shown in Figure 2.2.

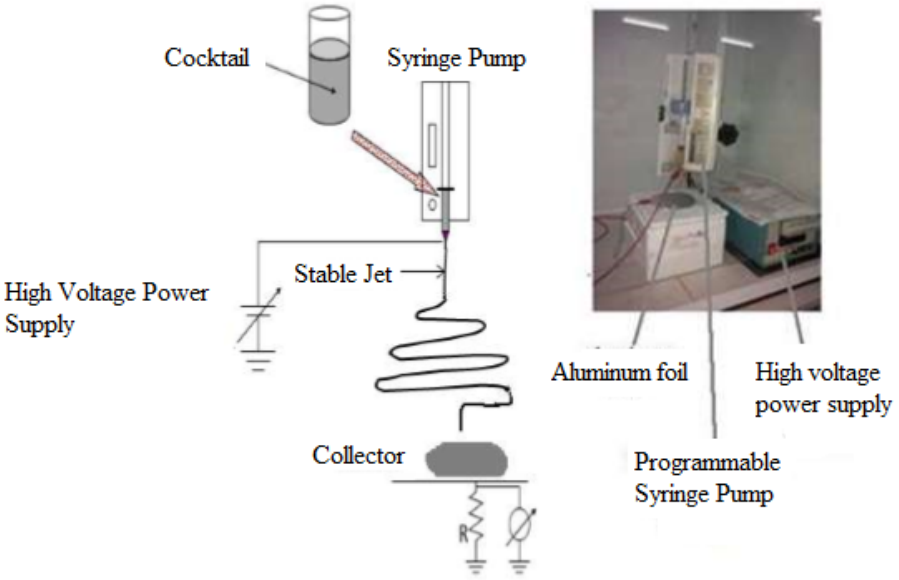

Figure 2.2 The commonly used electrospinning set-up

2.5.3 Time Correlated Single Photon Counting (TCSPC) Apparatus

Fluorescence lifetimes were recorded using a Time Correlated Single Photon Counting (TCSPC) system that was from Edinburgh Instruments (UK). The instrument was equipped with a 467 nm pulsed laser (pulse width: 79 picoseconds) as the excitation source. All lifetimes were calculated using the software of the instrument and fit to a $\chi 2$ value of less than 1.7 and the residuals trace symmetrically distributed around the zero axes.

CHAPTER THREE
INTRODUCTION

3.1 Introduction

Contamination of the waters with silver ions has become an important issue due to the increasing use of silver in many fields on technology; industry and medicine. Today, ionic or metallic forms of silver are found in environmental water samples, pool water, water purification related samples, residues from bio-films, dental treatment water, integrated textile products like wound healing bandages and even in washing machines and refrigerators. This intensive interest towards silver and use of soluble silver formulations causes over exposure to silver compounds. However, the Environmental Protection Agency (EPA) bring some limitations for the allowed concentrations of Ag(I) which is lower than 1.6 nM for the aquatic life and less than 0.9 mM in drinking water (EPA, 1980). Therefore, correct and sensitive analysis of trace amounts of ionic silver is a target research topic. Up to now many different analytical techniques including atomic absorption spectrometry (AAS), inductively coupled plasma-mass spectrometry (ICP-MS), electrochemical applications and spectrofluorimetric approach have been used for detection of ionic silver in the analysis of a variety of samples including biological and environmental species (Ongun Zeyrek, Ertekin, Nadeem, & Birel, 2016). Fluorescence-based detection methods have some advantages over others due to the selectivity, sensitivity, and simplicity. Most of the fluorescent based sensing techniques use fluorescent dyes in solution or in immobilized form, in solid state. Up to now a number of fluorescent chemosensors for silver ion have been designed and tested successfully (Coskun, & Akkaya, 2005; Kandaz, Güney, & Senkal, 2009; Iyoshi, Taki, & Yamamoto, 2008; Shamsipur, Alizadeh, Hosseini, Caltagirone, & Lippolis, 2006; Wang, Xue, Qian, & Jiang, 2010; Topal, Gürek, Ertekin, Yenigul, & Ahsen, 2010; He, Song, Wang, Shi, & K. Chen, & G.R. Chen, 2011; Wang, Xue, Qian, & Jiang, 2010; Kacmaz, et all., 2011).

Table 3.1 compares most of the previous studies on the determination of Ag^+ ions in terms of the sensing material, analysis moiety, working range, limit of detection (LOD), and selectivity (Ongun Zeyrek, Ertekin, Nadeem, & Birel, 2016).

According to the literature information, in recent works studies performed in solid state are more than the studies in solvent phase. Additionally, they present better detection limits (Topal, Gürek, Ertekin, Yenigul, & Ahsen, 2010; Kacmaz, et al., 2011) with respect to the solution phase studies.

Herein we have successfully utilized the solid state materials for detection of very low concentrations of silver utilizing the electrospun fiber materials. In this study, matrix materials of poly (methyl methacrylate) (PMMA) and ethyl cellulose (EC) were used to encapsulate the silver sensing dye. The fluorescent probe:

(1,4-phenylenebis(azaneylylidene))bis(methaneylylidene))bis(N,N-dimethylaniline) was used as the indicator. The dye exhibited strong absorbance and bright luminescence.

To the best of our knowledge this is the first attempt using the Y-10 dye as the fluoroionophore-along with electrospinning approach for silver sensing at sub-nanomolar levels.

Table 3.1 Former studies on the determination of Ag (I) ions in terms of the chemosensor, analysis media, working range, detection limit, and selectivity

Silver sensing Agent	**Matrix material /Response**	**Working range**	**LOD**	**Stability/Reversibility Selectivity**	**Ref No**
Boradiazaindacenes, (λex, 480 nm)	Solution phase, THF	Ag^{+} (0- 10 μM)	-	No interference for $Pb^{2+,}$ Hg^{2+} Co^{2+} $Mn^{2+}$and Fe^{2+},	(Coskun, & Akkaya, 2005)
zinc-phthalocyanine bearing benzofurane structure (λex 345 nm, 616 nm).	Solution phase, THF/Quenching based sensor	1.0-50 μM Ag^{+}	-	-	(Kandaz, Guney, & Senkal, 2009)
Rosamine based fluorescent probe , λex = 520 nm.	Solution phase Ethanol	0.0-5.0 μM Ag^{+}	10^{-7} M Ag^{+}	Selectivity over Hg^{2+}, Pb^{2+}, Na^{+}, Mg^{2+}, Ni^{2+}, Fe^{3+} Zn^{2+} $Cd^{2+}$and Cu^{2+}.	(Iyoshi, Taki, & Yamamoto, 2008)

Table 3.1 continues

Bis-pyrene dye with two pyridines (λex = 344 nm)	Solution phase Ratiometric response in DMSO-HEPES	0.0-20 μM Ag^{+}	-	Selectivity over Al^{3+}, Ca^{2+}, Cd^{2+}, Co^{2+}, Cu^{2+}, Fe^{2+}, Fe^{3+}, Hg^{2+}, K^{+}, Li^{+}, Mg^{2+}, Zn^{2+},Na^{+}, Ni^{2+}, Pb^{2+}, Sr^{2+}, and Mn^{2+}	(Wang, Xue, Qian, & Jiang, 2010)
Zn (II) phthalocyanines ((λex) 640, (λem) 717 nm)	Solid state Ethyl cellulose (EC) (Thin Film Form)	10^{-10} -10^{-4} M Ag^{+}	7.6×10^{-12} and 2.3×10^{-11}M	No interference for Sb^{3+}, Al^{3+}, Bi^{3+}, Li^{+}, Hg^{2+}, Pd^{2+},Zn^{2+}, Cu^{2+}, Ni^{2+}, Co^{2+}, (Stabel At least 180 days)	(Topal, Gürek, Ertekin, Yenigul, & Ahsen, 2010)
Bis-triazolocoumarins ((λex) 345, (λem) 400-550 nm	Salty water Fluorescence quenching based sensor	Ag^{+} (0-10 μM)	-	High sensitivity, no cross sensitivity towards Mg^{2+}, Ca^{2+}, Mn^{2+}, Ni^{2+},$Zn^{2+}Cu^{2+}$, Co^{2+}, Cd^{2+}, Na^{+}, K^{+}.	(He, Song, Wang, Shi, Chen, & Chen, 2011)

Table 3.1 continues

Azacrown dye (λex) 380 nm) λem 519 nm	Ethanol	-	-	High sensitivtiy for Ag^{+}, No cross sent. For (Cr^{3+}, Fe^{3+}, Cu^{2+}, and $Pb^{2+,}$, slight sensitivty for Ca^{2+}, Mg^{2+}, Co^{2+}, Ni^{2+}, Hg^{2+}, Zn^{2+}, Cd^{2+}, K^{+}, Mn^{2+})	(Wang, Xue, Qian, & Jiang, 2010)
(1,2-bis(4-methoxybenzylidene) hydrazine) dye	poly(methyl methacrylate) PMMA, EC Electrospun nano fiber	10^{-12} -10^{-6} M Ag^{+}	-	No interference for Li^{+}, Na^{+}, K^{+}, Ca^{2+}, Ba^{2+}, Mg^{2+}, NH_4^{+}, Pb^{2+}, Al^{3+}, Cr^{3+},Mn^{2+}, Sn^{2+}, Hg^{+}, Hg^{2+}, Fe^{2+} and Fe^{3+} Ni^{2+}, Co^{2+}, Cu^{2+}, No selectivity for NO_3^{-}, NO_2^{-}, F^{-}, Cl^{-}, Br^{-}, SO_4^{2-} and PO_4^{3-}	(Kacmaz, et al., 2011)
Fluorescently labeled single-stranded DNA	MOPS buffer	0-400 nM Ag^{+}	1 nM Ag^{+}	Selectivity over Ca^{2+}, $Mn^{2+,}$ Ni^{2+}, Pb^{2+}, Cd^{2+}, Co^{2+}, Cu^{2+}, Fe^{2+}, Fe^{3+}, Mg^{2+}, and Zn^{2+}.	(Lang, Li, Huang, Yu, & Chen, 2016)

Table 3.1 continues

Graphene oxide the self-hybridization of cytosine-rich ss-DNA labeled with the fluorescent tag FAM in presence of Ag(I)	-/Strong amplification of fluorescence.	1–250 nM	0.1 nM	Selectivity over Cu^{2+}, Hg^{2+}, Co^{2+}, Cd^{2+} Fe^{3+}, Zn^{2+}.	(Sun, Lai, Lin, Huang, Zuo, & Lia, 2016)
Fluorescent probe (E)-3,6-bis (allyloxy)-2-((thiazol-2-ylmethylene)amino) -4a,9a-dihydrospiro[isoindoline-1,9-xanthen]-3-one	Detection at 490 nm / Solution phase pH 7.4	10 to 60 μM	-	Selectivity over Ni^{2+}, Pb^{2+}, Zn^{2+} , Co^{2+}, Cu^{2+}, Fe^{2+} ,Al^{3+}, Ba^{2+}, Ca^{2+}, Hg^{2+}.	(Langhals, Ismael, & Yuruk, 2000)

Table 3.1 continues

Perylenediimide dye in ethyl cellulose and poly(methyl methacrylate)	Fluorescence quenching, Detection at 490 nm /	10^{-9}-10^{-3} M [Ag^{+}] in DCM-EtOH and 10^{-10}-10^{-5} M Ag^{+} in solid state	2.6×10^{-10} and 4.3×10^{-11}M [Ag^{+}] for solution and solid state, respectively	Selectivity over Ca^{2+}, Ba^{2+}, Li^{+}, Na^{+}, K^{+}, Mg^{2+}, NH_4^{+}, Ni^{2+}, Co^{2+}, Mn^{2+}, Sn^{2+}, Cu^{2+},Pb^{2+}, Al^{3+}, Cr^{3+}, Hg^{+}, Hg^{2+}, Fe^{2+} and Fe^{3+} ions	(Ongun, Ertekin, Nadeem, & Birel, 2016)
Phenazine derivative	Fluorescence quenching, at 415 nm ON-OFF fluorescent switch	0.07 µM Ag(I)	-	Selectivity over Fe^{3+}, Hg^{2+}, Ag^{+}, Ca^{2+}, Cu^{2+}, Co^{2+}, Ni^{2+}, Cd^{2+}, Pb^{2+}, Zn^{2+}, Cr^{3+}, and Mg^{2+}	(Wei, et al., 2017)
Multivalent calix[4]arene-based fluorescent sensor	Fluorescence shift toward Ag^{+} in aqueous methanol	Assosication constant Ka=5818710.74 M^{-1})	-	high recognition efficiency of the dye in physiological medium	(Lotfi, et al., 2017)

Table 3.1 continues

Fluorescence chemosensor based on biomolecular peptid DP (Dansyl-Leu-Leu-Cys-Acp-Asp-OH)	Ag^+ and H_2S sensing in 100% aqueous solution and living cells	Ag^+ in the concentration range of 0–10μM	Detection limits of 61.7nM and 74.0nM for Ag+ and H2S, respectively.	Ag Selectivity over (Hg^{2+},K^+, Na^+, Ca^{2+}, Cd^{2+}, Co^{2+}, Cr^{3+}, Cu^{2+}, Mg^{2+}, Mn^{2+}, Ni^{2+}, Pb^{2+}, Zn^{2+}, Al^{3+}, Fe^{2+}, Fe^{3+}) and most of the anions.	(Su, et al., 2018)
di-4-(2-quinolinylhydrazinyl)diphenyl sulfone	Weak blue fluorescence in THF/a strong emission in aggregated state	(LOD = $2.0x10^{-7}$ mol/L)	Binding constant of K = 1.58 9 10^{10} (mol/L)-2.	Selective Ag(I) over Al, Ba^{2+} $Ca^{2+,}$ $Cd^{2+,}$ $Co^{2+,}$ Cr^{3+}, $Cu^{2+,}$ Fe^{2+}, Fe $^{3+}$, Hg^{2+}, K^+, Mg^{2+}, Mn^{2+}, Ni^{2+}, Pb^{2+}, Sn^{2+} and Zn^{2+}	(Gong, Yang, Zhang, Zhou, & Xue, 2018)
3-indolyl-4-indazolyl maleimide derivatives	In EtOH, DCM, DMF, THF, toluene, and chloroform	Ag^+ in the concentration range of ($2.0x10^{-6}$–$2.0x\ 10^{-5}$ mol/L	-	Selective ratiometric (bathochromic) Ag^+ over Li^+, Cu^{2+}, Zn^{2+}, Hg^{2+}, Ni^{2+}, Al^{3+}, Fe^{3+}, and Cr^{3+}.	(Zhu, et, all., 2018)
Chemosensor 4-dimethylaminocinnamaldehyde for detection silver(I) and sulfide.	dimethylformamide (DMF)	Amounts of 0.8–10.6μl of a stock $AgNO_3$ solution (10mM) in DMF	-	Al^{3+} and Fe^{2+} decreased the fluorescence intensity of dye,and Cu^{2+}, Ga^{3+},In^{3+} and Hg^{2+} quenched it. Only bathochromic shift from 449 to 488nm of Ag^+.	(Kang, Byeong, & Kim, 2018)

Table 3.1 continues

Coumarin-based chemosensor for colorimetric detection of Ag(I) ion and fluorogenic sensing of Ce(III) ion	In aqueous solution in ($EtOH/H_2O$)	-	-	The color of silver changed from pale yellow to brown and the spectrum also changed. No change in other metals (Cu^{2+}, Hg^{2+}, Zn^{2+}, Li^{+}, Na^{+}, Al^{3+}, Fe^{3+}, Co^{2+}, Ni^{2+}, K^{+} and Cr^{3+}) was observed.	(Liu, Xu, Song, Li, & Xian, 2018)
S, N-doped carbon quantum dot-based "off-on" fluorescent sensor for silver ion and cysteine (Cys)	İn phosphate buffer Off-on fluorescence probe	Linear range of 0–10 and 10–250μM	Detection limit of detection 0.40μM for Ag^{+} and (Cys) respectively	-	(Liao, et al., 2018)

Table 3.1 continues

Bifunctional supramolecular pseudorotaxane chemosensor (G-WAP)	DMSO/ H_2O (1:1, v/v)	Concentration of Ag^+ ($1x10^{-4}$ M, 0.0–3.0 equiv.)	The detection limits of G-WAP for Ag^+ is $1.2x10^{-8}$ M, for Hg^{2+} is $5.0x10^{-7}$ M	The real-time fluorescence response did show excient quenching of the supramolecular pseudorotaxane chemosensor (G-WAP) upon the addition of Ag^+ and showed an obvious fluorescence color change of the supramolecular pseudorotaxane chemosensor (G-WAP) upon the addition of Hg^{2+}	Zhang, et al., 2018)
(1, 4-phenylenebis(azaneylylidene))bis(methaneylylidene))bis(N,N-dimethylaniline)	Thin film electrospun fibers fluorescence quenching and florescence enhancement	Working range Ag^+ ($1x10^{-12}$-$1X10^{-4}$ M)	The detection limits of Ag(I) is $1.1x10^{-15}$ M.	Selective Ag over Al^{3+}, Ca^{2+}, Cu^{2+}, Fe^{3+}, Hg^{2+}, K^+, Mg^{2+}, $Mn^{2+}$and Pb^{2+},	This work

3.2 Spectral Characterization of the Dye

3.2.1 UV-visible Based Spectral Data of the Dye

The UV visible spectra of the utilized dye were recorded in the solvents of ethanol (EtOH), tetrahydrofurane (THF), dicloromethane (DCM) and in solid matrix of ethyl cellulose (EC), respectively. The solid state measurements were performed both ionic liquid free (IL-free) and ionic liquid doped (IL-doped) matrices. In all of the studied moieties the dye exhibited strong absorbtion bands centered on 390 nm when tested in the solvents. However, when encapsulated in EC, the absorption band centered at 477 and 483 nm for the IL-free and IL-doped matrices, respectively (Table 3.2).

Table 3.2 Reveals absorption based charecteristics of the Y10 dye in different moieties

DYE	Solvent Matrix	λ_1 abs(nm)	λ_2 abs(nm)	E_{max} (λ_1 abs) ($M^{-1}xcm^{-1}$)	E_{max} (λ_2 abs) ($M^{-1}xcm^{-1}$)
Y10	EtOH	390	-	24700	-
Y10	THF	390	-	29000	-
Y10	DCM	391	-	35000	-
Y10 (IL FREE)	EC	340	477	$3,2X10^5$	$2.2X10^5$
Y10(IL)	EC	-	483	-	$5,08x10^5$
Y10(IL-FREE)	PVC	410	480	$3,0X10^5$	$2,4X10^5$

3.2.2 Emision Based Studies

Herein we recorded the excitation and emission spectra of the Y10 dye in THF, EC, PMMA and PVC, respectively. Figure 3.1 (I) and (II) reveals gathered excitation-emission spectra of the dye in different moieties. The dye can be excited by the 466, 464, and 453 nm in the EC, PMMA and PVC, respectively. Emission can be acquired at 528, 550 and 610 nm, in the same order for the used polymeric matrices. The Stoke's shift values of 62, 86 and 157 nm can be extracted for the EC, PMMA and PVC, respectively. In spite of the smallest Stoke's shift we have chosen the EC matrix for the further studies due to the superior ion diffusibility and high relative signal change dynamics (Table 3.3).

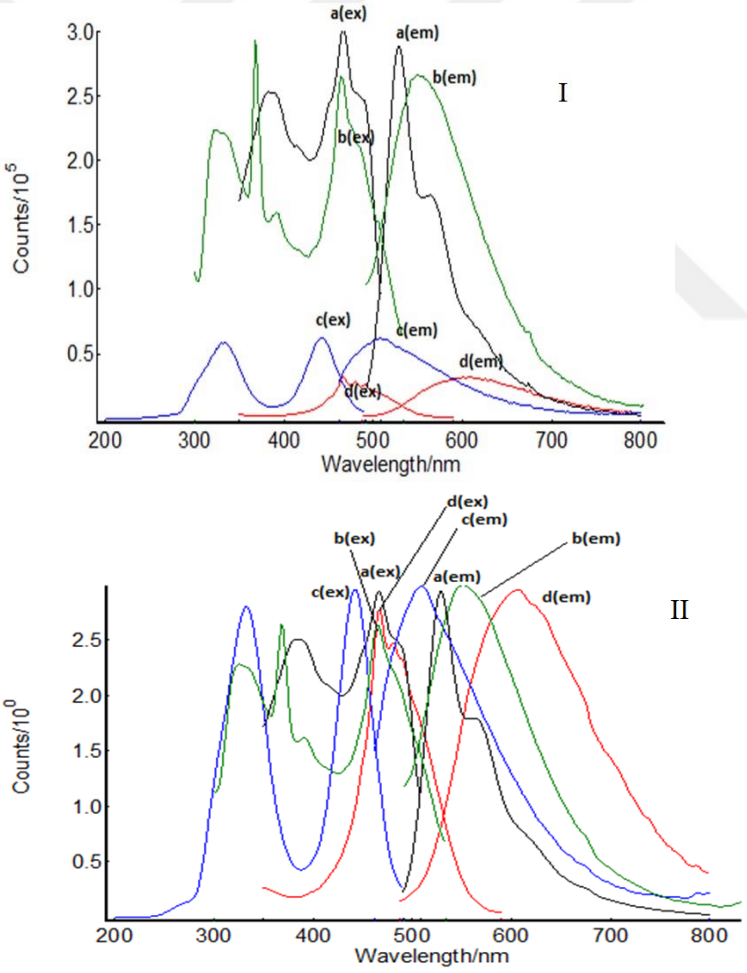

Figure 3.1 I. Excitation and emission spectra of the Y10 dye. (a) EC, (b) PMMA, (c) THF, (d) PVC. II. Corrected excitation and emission spectra of the Y10 dye in the same moieties

Table 3.3 Excitation Emission spectral data of the Y10 dye in different moities. λ^{em}_{max}: emission maximum, λ^{ex}_{max}: excitation maximum, $\Delta\lambda_{ST}$: Stoke's shift

Compound	Matrix	λ^{em}_{max}	λ^{ex}_{max}	$\Delta\lambda_{ST}$ (Stoke's shift)
Y10 IL-free	THF	442	332	110
	PMMA	550	464	86
	PVC	610	453	157
	EC	582	466	116
Y10 IL-doped	EC	528	466	62

3.2.3 pH Dependency of the Dye

pH dependency of the dye has been tested in the THF for the pH range of 2.0-7.0 and 7.0-12.0, respectively. The pH values were adjusted to the desired pH titrating by 10^{-3} M solutions of HCI or NaOH. Figure 3.2 and 3.3 show the pH dependent spectral variations for the acidic (pH= 2.0-7.0) ranges. Figure 3.4 and 3.5 show the pH dependent spectral variations for the alkaline (pH= 7.0-12.0) ranges.

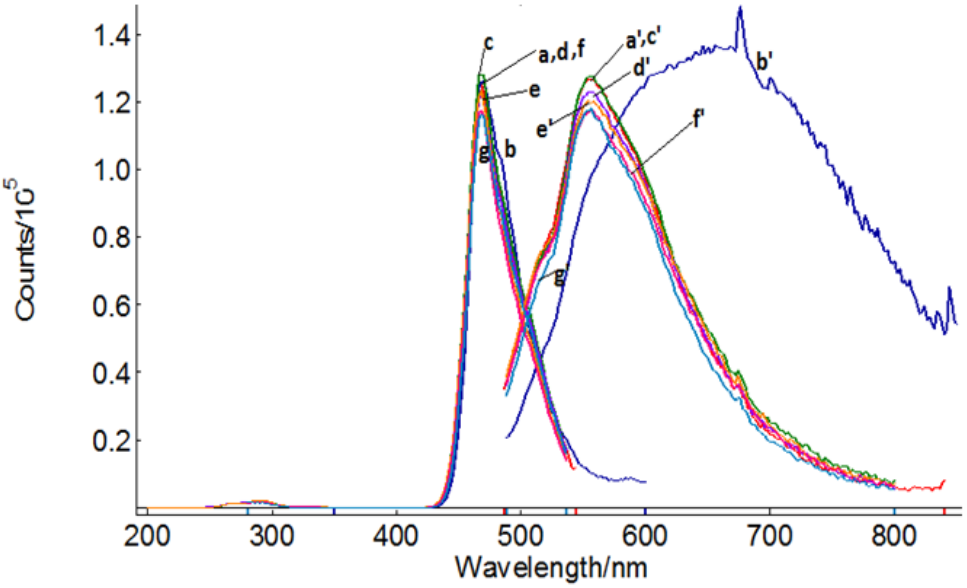

Figure 3.2 pH dependency of the Y10 in THF between pH 2.0-7.0 λmax ex 468, λ max em 556 nma-a': in THF, b-b': pH 2.0 , c-c': pH 3.0 d-d': pH 4.0 e-e': pH 5.0 f-f': pH 6.0 g-g': pH 7.0

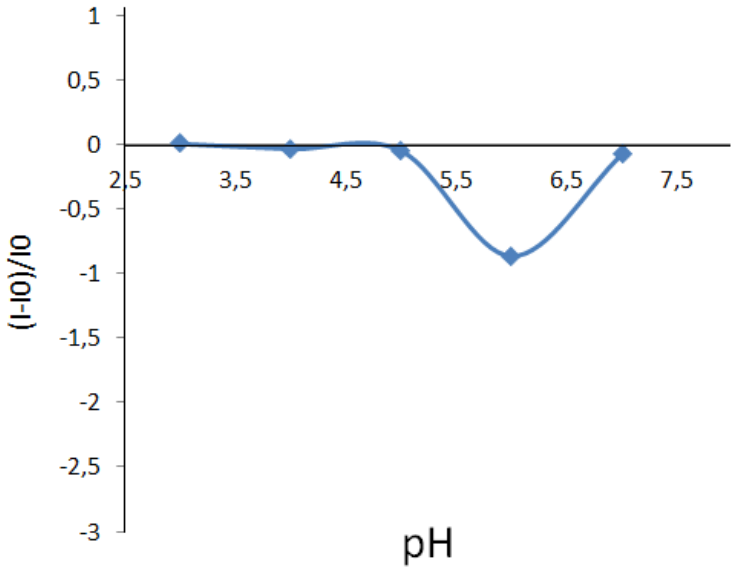

Figure 3.3 Dependency of the signal $((I-I_0)/I_0)$ of Y10 to pH in THF between pH 3.0-7.0

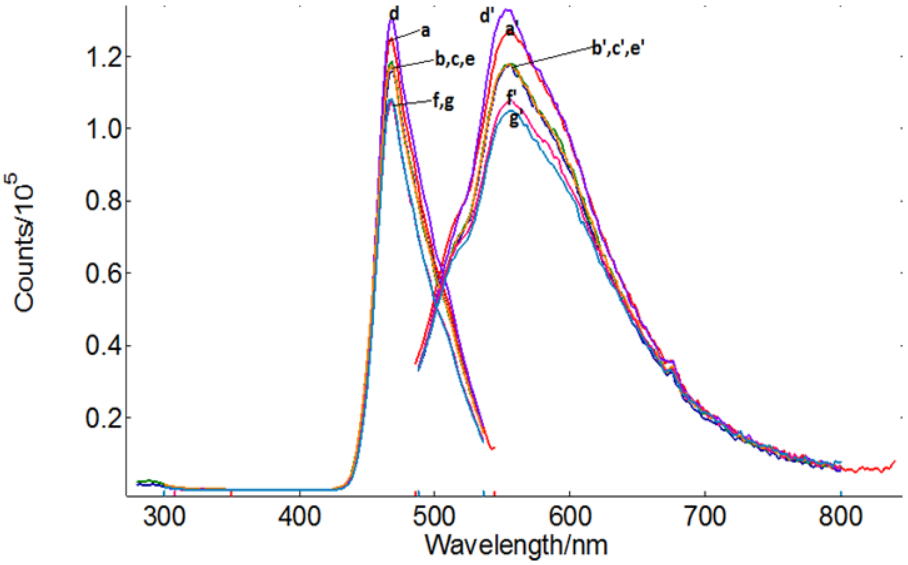

Figure 3.4 pH dependency of the Y10 in THF between pH 7.0-12.0 λ_{max}^{ex} 468, λ_{max}^{em} 556 nma-a': in THF, b-b': pH 7.0 , c-c': pH 8.0, d-d': pH 9.0, e-e': pH 10.0, f-f': pH 11.0, g-g': pH 12.0

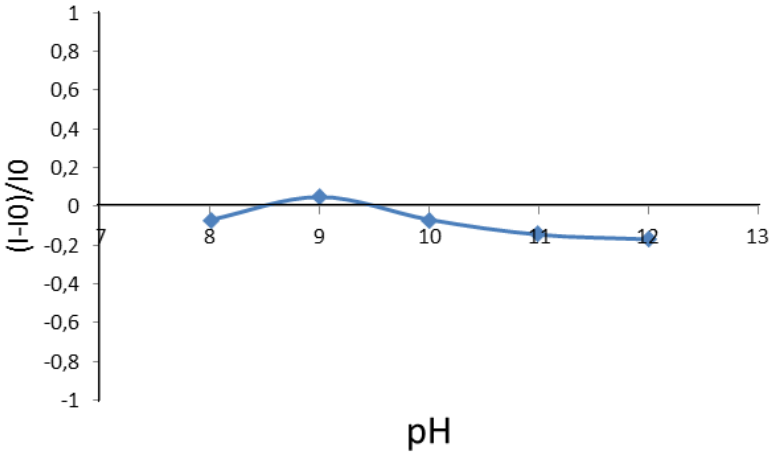

Figure 3.5 Dependency of the signal ($(I-I_0)/I_0$) of Y10 to pH in THF between pH 8.0-12.0

According to the Figure 3.4 and 3.5 it can be concluded that pH dependency of the dye is very limited near neutral region of the pH scale. Therefore we have chosen the pH of 7.0 for further studies. We tested the ion sensitivities of the dyes towards silver and other ions in phosphate buffered solutions around pH 7.0.

3.3 UV-based Response of the Y10 Towards Ionic Silver

UV based response of the EC encaptulated Y10 dye has been investigated both for IL-free and IL-doped composites on thin films for a large concentration range of

10^{-12}- 10^{-5} M. Figure 3.6 (I) and (II) reveals variation of the UV spectra of dye doped thin films upon exposure to the different concentrations of Ag (I) solutions at pH 7.06.

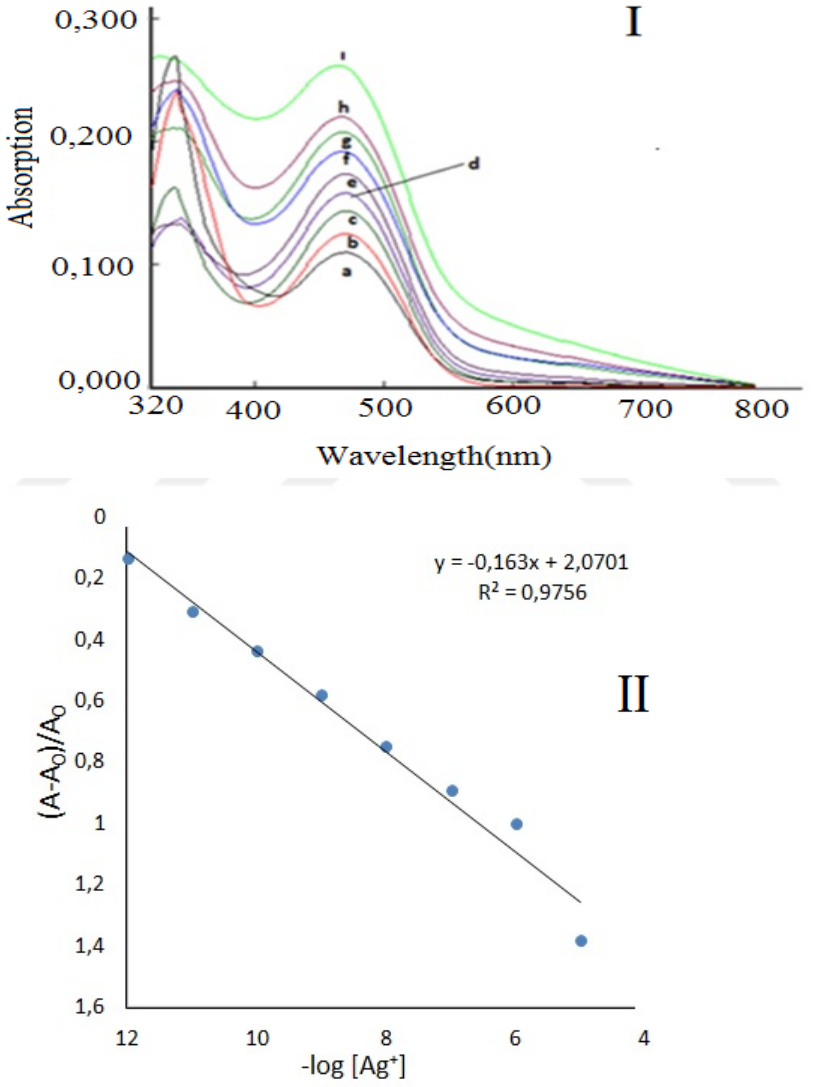

Figure 3.6 I: Variation of the UV-Vis. spectra of IL-free thin films upon exposure to the different concentrations of Ag (I) solutions at pH 7.06. (a) Ag free buffer, (b) 10^{-12} M, (c) 10^{-11} (d) 10^{-10}, (e) 10^{-9} , (f) 10^{-8} , (g) 10^{-7} , (h) 10^{-6} , (ı) 10^{-5} M Ag(I). II: Linearized calibration plot for the concentration range 10^{-12}- 10^{-5} M Ag(I)

In the absence of the ionic liquid the EC doped Y10 dye exhibited an enhancement in the absorption integral when exposed to increasing concentrations of the Ag (I). This can be concluded as an evidence of a complex formation between the dye and the Ag (I). Contrary, the ionic liquid doped composites exhibited a decrease in the absorption intensity when exposed to silver solutions. This contraversial finding observed in the UV based spectral response of the IL-doped and IL-free composities can be interpreted as presence of two different mechanisms.

Figure 3.7 (I) and (II) reveals variation of the UV-Vis. spectra of the IL containing dye doped thin films upon exposure to the different concentrations of Ag(I) solutions at pH 7.06.

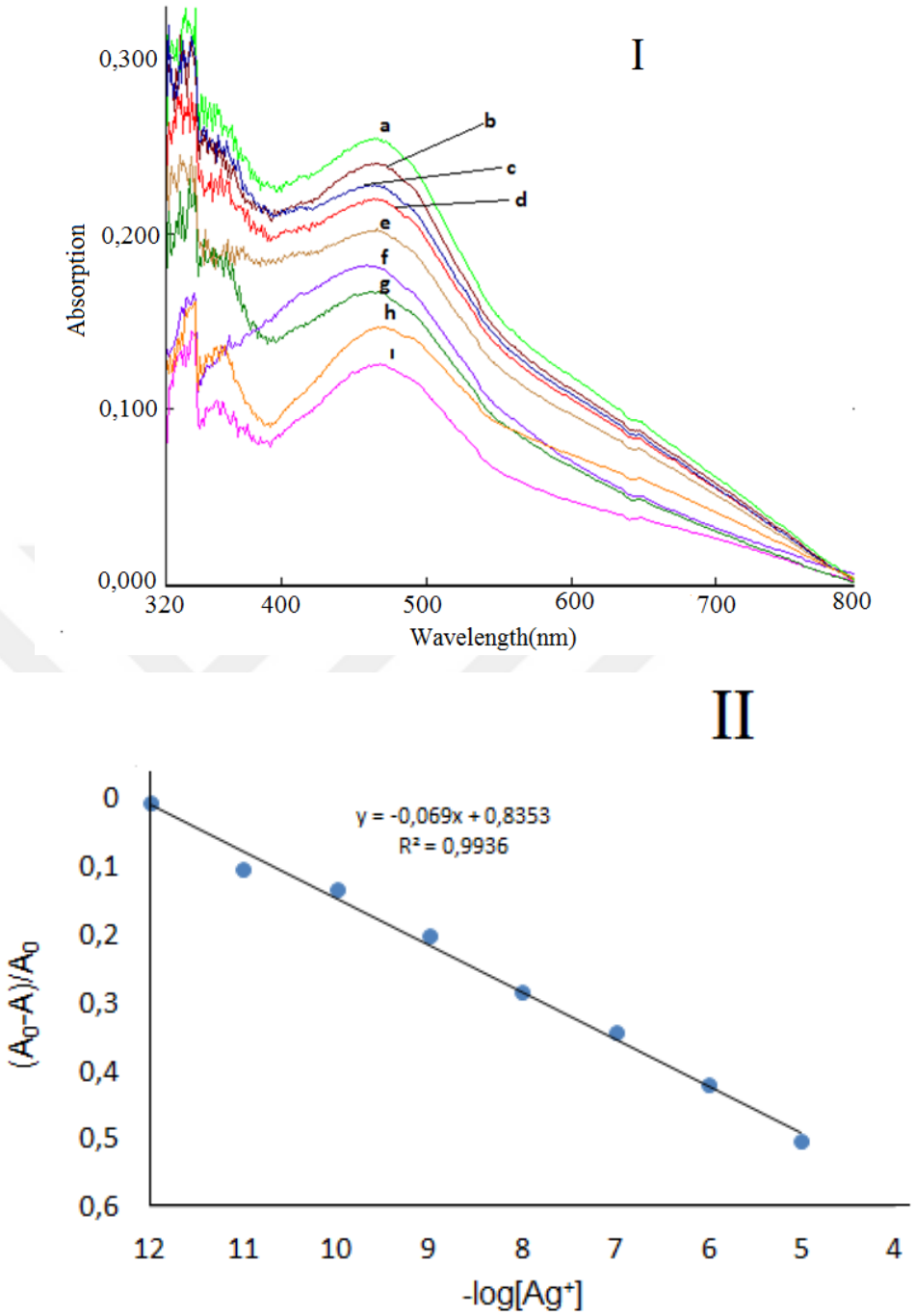

Figure 3.7 I. Variation of the UV-Vis. spectra of IL-doped thin films upon exposure to the different concentrations of Ag (I) solutions at pH 7.06. . (a) Ag free buffer, (b) 10^{-12} M, (c) 10^{-11} (d) 10^{-10} , (e) 10^{-9} , (f) 10^{-8} , (g) 10^{-7} , (h) 10^{-6} , (ı) 10^{-5} M Ag(I). II: Linearized calibration plot for the concentration range 10^{-12}- 10^{-5} M Ag(I)

3.4 Emission Based Response Towards Ag(I) Ions

3.4.1 Response of Thin Films

Emission based response of the Y10 dye was tested both for thin film and elecrospun forms. Additionally, IL-free and IL-doped composites of each form were tested for silver ion sensitivity. The thin film forms of the IL-free composities exhibited a decrease in signal intensity at 580 nm for the contentration range of 10^{-12}-10^{-8} M [Ag^{+}]. However, the IL-doped thin films exhibited a signal enhancement upon exposure to the silver ions for a larger of contentration range of 10^{-12}-10^{-4} M. Calibration plots of the regarding spectra were shown in Figure 3.8 and 3.9 for the IL-free and IL-doped thin films, respectively.

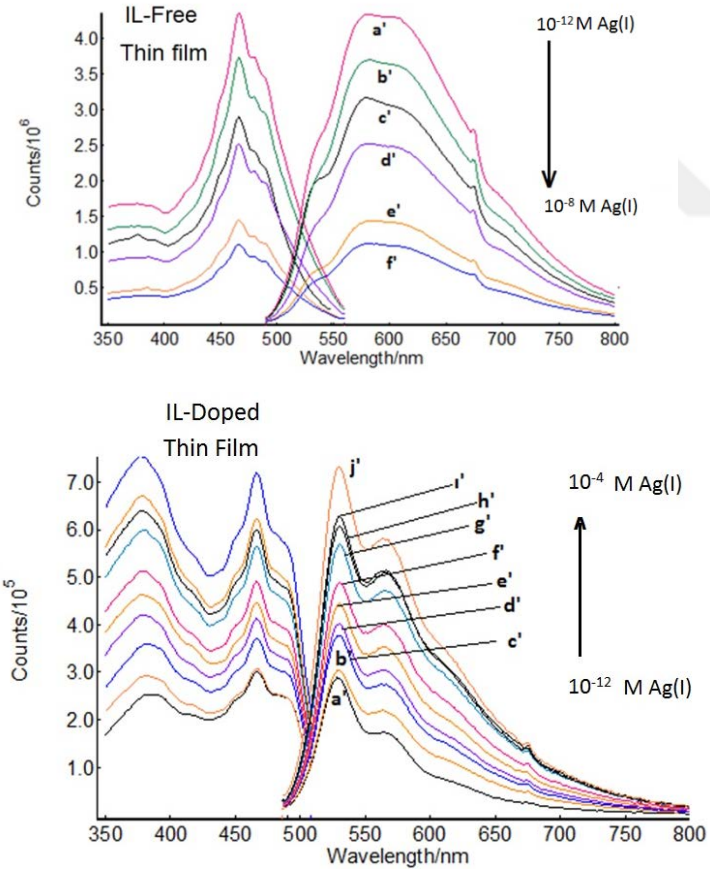

Figure 3.8 Spectral response of the IL-free and IL-doped dyes in EC matrix in thin film forms towards Ag^{+} ions at pH 7.0. (a') Ag free buffer, (b') 10^{-12} M, (c') 10^{-11} , (d') 10^{-10} , (e') 10^{-9} , (f') 10^{-8} , (g') 10^{-7} , (h') 10^{-6} , (ı) 10^{-5} , (j) 10^{-4} M Ag (I)

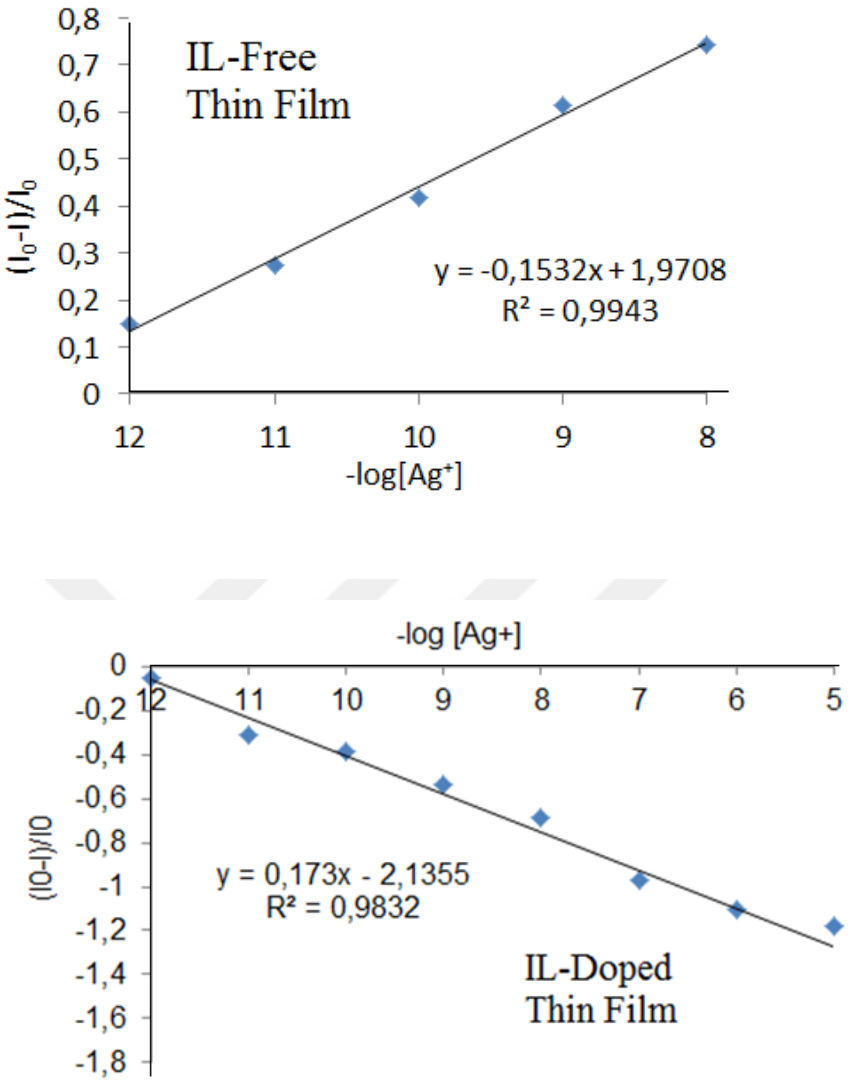

Figure 3.9 Calibration plot for the IL-free and IL-doped thin film forms of the Y10 dye after exposure to certain concentrations of ionic silver. IL-free thin film: 10^{-12}- 10^{-8} M Ag(I), IL-doped thin film: 10^{-12}- 10^{-5} M Ag(I)

Calibration plots of the IL-Free and Doped thin films exhibited different characteristics in terms of the slops.

The “y” axess is the corrected intensity ratio of metallated (I) and metal-free (I_0) forms of the indicator, (I_0-I)/I_0. The linearized calibration plot of the IL-free sensing slide can be described by, y= -0.1532x+1.9708 and the correlation coefficient of R^2= 0.9943. However, the IL-doped composites yielded calibration plot of y= 0.173x-

2.1355 and R^2 value of 0.9832. From the slops of the calibration plot it can be concluded that, both of the composites can be used for the sensing of sub-nanomolar concentrations of the ionic silver in phosphate buffered solutions. However, the IL-doped formulation is superior due to the larger concentration range and higher slop with respect to the IL-free composites.

As mentioned earlier presence of the IL in the sensing composites resulted with opposite characterictics in the direction of signal intensity in the excitation-emission spectra of the Y10. Similar behavior was also observed in the UV-vis. spectra. In this case both the emission and absorption based response should be evaluated together to clarify the mechanism behind this behavior. As the absortion intensity increasing the decrease observed in the excitation-emission intensity may be an indicator of a complex formation between the dye and the Ag^+ ions in the IL-free forms. However, this possiblty should be supported by decay time measurements. On the other hand, in case of the IL-doped forms, while the absorption based signal intensity decreasing, the excitation-emisssion signals exhibited an enhancement which can be attiributed to the presence of a different mechanism from the IL-free forms.

3.4.2 Response of Electrospun Fibers

Excitation-emission based spectral data were also acquired for the electrospun fibers. The IL-free and IL-doped fibers exhibited similar response with the thin films in terms of the signal direction. While the IL-free forms exhibiting a signal drop at 579 nm, the IL-doped forms displayed an enhancement in the signal at 588 nm. Both the IL-free and IL-doped fibers worked for the concentration range of 10^{-12}-10^{-9} and 10^{-12}-10^{-8} M Ag (I), respectively (Figure 3.10 and 3.11). Detection limit of Y10 doped sensing film was found to be $1.1x10^{-15}$ M for Ag^+ (LOD concentration of the metal ion giving a signal equal to average of the balank signal (for n=20) plus three standard deviations).

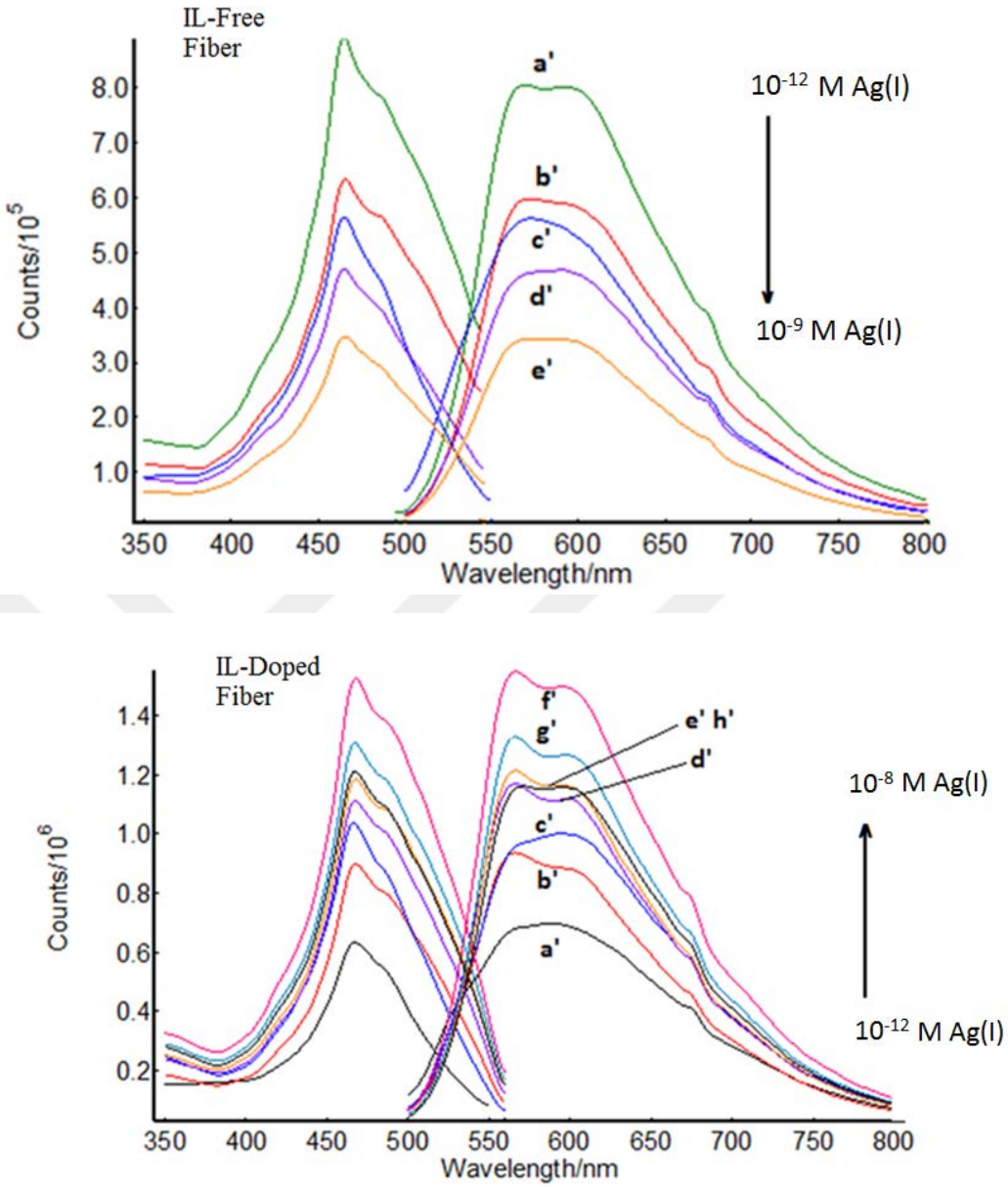

Figure 3.10 Spectral response of the IL-free and IL-doped electrospun fibers in EC matrix towards Ag^+ ions at pH 7.0. (a') Ag free buffer, (b') 10^{-12} M, (c') 10^{-11} , (d') 10^{-10} , (e') 10^{-9} , (f') 10^{-8} , (g') 10^{-7} , (h') 10^{-6} Ag (I)

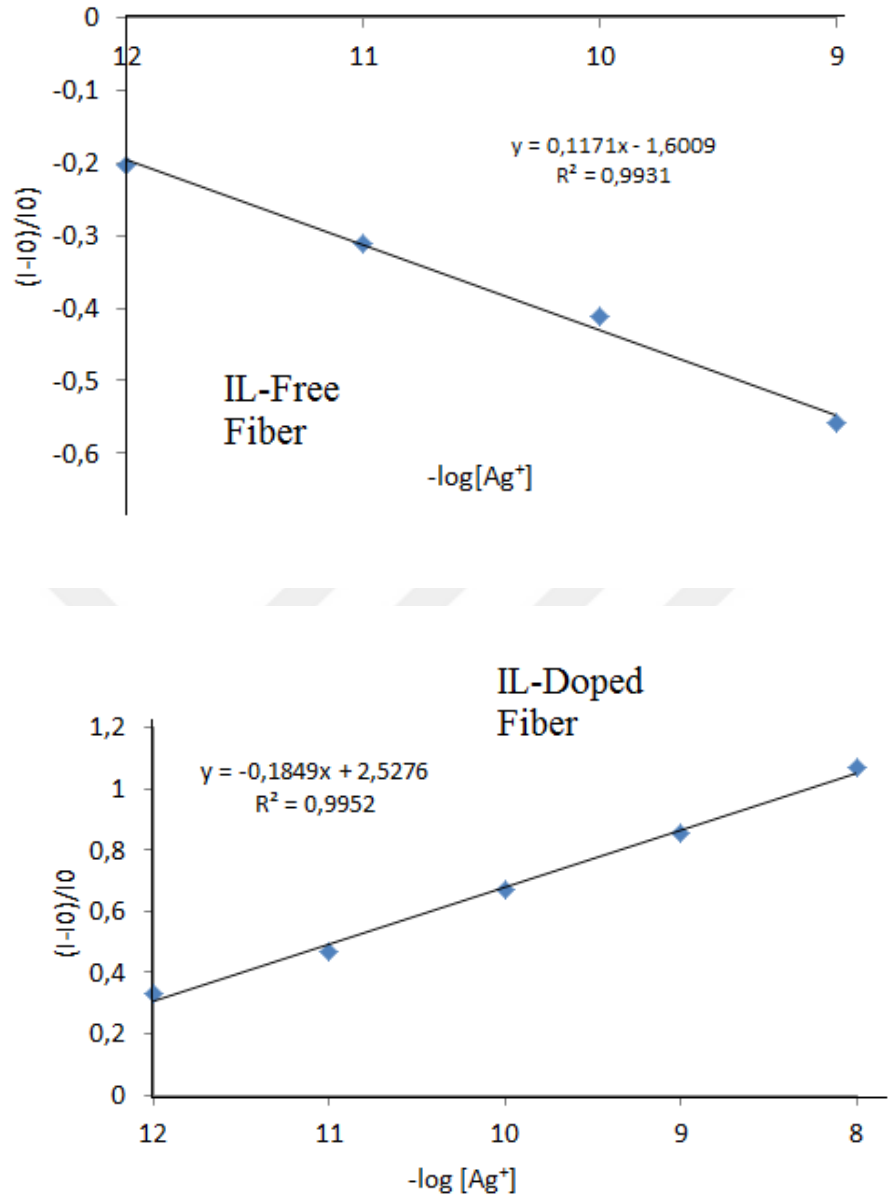

Figure 3.11 Calibration plot for the IL-free and IL-doped electrospun fibers of the Y10 dye after exposure to certain concentrations of ionic silver. IL-free thin film: 10^{-12}-10^{-9} M Ag(I), IL-doped thin film: 10^{-12}-10^{-8} M Ag(I)

Figure 3.10 and 3.11 reveal excitation-emission spectra and calibration plots of the electrospun fibers of the Y10 dye. The electrospun fibers have been saturated at lower concentrations of the silver with respect to the thin films. While the IL-free thin films responding for the concentration range of 10^{-12}- 10^{-8} M Ag(I), the IL-doped forms responded between 10^{-12}-10^{-9} M Ag(I). Similarly, the working range of

the electrospun fibers appeared between 10^{-12}-10^{-9} M and 10^{-12}-10^{-8} M Ag(I) for the IL-free and IL-doped fibers, respectively. In spite of the narrow working ranges the electrospun fibers exhibited better slope and R^2 values with respect to the thin films.

3.5 Decay Time Measurements

The fluorescence lifetimes were recorded in thin films in the absence and presence of the ionic liquid prior and after exposure to 10^{-3} M solutions of ionic silver. During lifetime measurements the sensing agents were excited with a laser light source (467 nm) and the emission related data were acquired at 580 and 528 nm for the IL-free and IL-doped forms, respectively. While the IL-free thin films exhibiting bi-exponential decays, the IL-doped forms displayed tri-exponential decay times. The bi-exponential decays varied between 0.64-0.66 ns for the short lifetime and between 1.88-3.44 ns for the long lived component. Table 3.4 reveals detailed information including % distribution of the components and statistics of the lifetime measurements.

In case of the IL-doped forms the tri-exponential decays varied between 0.62-0.82 ns for the shortest lifetime and between 4.34-13.00 ns for the longest lifetime component.

The multi exponential characteristic of the decay times can be attributed to the structural properties of the matrix, micro environment of the dye and the accessibility difficulties of the quencher to the sensing sites during lifetime measurements.

The average thicknesses of the used films were (5.17 μm±0.09 (n=10)) which may be effective on the diffusion of the quencher ions.

The average decay times of 0.85 and 0.80 ns for the IL-free and 2.71 and 2.35 ns for the IL-doped forms, prior and after exposure to 10^{-3} M of Ag^+ solution, respectively. Presence of the ionic liquid within the matrix approximatly three times increased the decay time of the dye.

In case of IL-free forms the decay time did not exhibit a significant change after exposure to Ag^+ ions (Table 3.4). However, in the IL-doped thin films, the average decay time decreased from 2.71 to 2.35 ns when exposed to the analyte.

When results of the steady-state and decay time measurements were evaluated together, the mechanisms behind the sensor signals can be explained better. In case of IL-free forms after interaction of the Y10 dye with Ag^+ ions a quenching has been observed in the emission spectra**.** The Stern-Volmer plots exhibited linear characterictics. Additionally herein the lifetime is unaffected by the presence of the quencher. Therefore this can be concluded as a pure static quenching.

However, in case of IL-doped forms we observed an enhancement in the fluorescence signal upon exposure to the silver ions which can be attributed to the fluorescence resonance energy transfer (FRET) between the IL and the Y10 dye. Herein we used significant amount of ionic liquid within the matrix which has an intrinsic fluorescence and probably acts as donor in our system.

Emission in imidazolium-based ionic liquids, in which the peak of the fluorescence spectrum shifts with the change in the excitation wavelength was reported earlier by Samanta and co-workers (Paul, Mandal, Samanta, 2005).

According to Cha, Shim, Ouchi, and Kim, the fluorescence spectrum of the 1-Butyl-3-methylimidazolium tetrafluoroborate [BMIM][BF4] violates Kasha's rule, which states that the fluorescence spectra of organic molecules should not change with a change in the excitation wavelength. Herein, the RTIL; [BMIM][BF4], when immobilized in EC matrix, acts as a donor in fluorescence resonance energy transfer. Binding of the silver ions to the Y10 dye enhances the FRET of the system. The variation of the avarega decay time from 2.72 to 2.35 ns and the long lifetime component from 13.00 to 4.34 ns can be concluded as an evidence of the FRET in this sensing scheme (Table 3.4).

Table 3.4 Revials decay times of the IL-free and IL-doped Y10 dye in the EC matrix

DYE	**MATRIX**	**10^{-3} M Ag^{+}**	**DECAY TIME(ns)**
Y10 (IL-free) Buffer Solution	EC	-	T_1:0.66±0.004(%83.95) T_2:1.88±0.05(%16.05) X^2:1.268 **T_{ave}:0.85**
Y10 (IL-free)	EC	+	T_1:0.64±0.04(%93.20) T2: 3.43± 4.28(%6.8) X^2:1.087 **T_{ave}:0.80**
Y10 (IL-doped) Buffer Solution	EC	-	T_1:0.82±0.016(%46.67) T_2:2.44±0.09(%43.61) T_3:13.00±2.18(%9.73) X^2:1.217 **T_{ave}:2.72**
Y10 (IL-doped)	EC	+	T_1:0.62±0.02(%18.92) T_2:1.89±0.004(%51.8) T_3:4.34±0.015(%29.9) X^2:1.682 **T_{ave}:2.35**

3.6 Selectivity Studies

In order to examine the response of the dye to possible interfering cations, the Y10 dye was treated with 10^{-3} M concentrations of Hg^{2+}, Al^{3+},Ca^{2+}, Cu^{2+}, Fe^{3+},K^{+}, Mn^{2+}, Mg^{2+}, Pb^{2+} ions in phosphate buffer solutions at pH 7.0. The chosen concentration for the potential interferents was 10^{6} fold of the ionic silver. The relative signal intensity changes caused by the potential interferent cations were shown in Figure 3.12. From Fig 3.12 it can be concluded that, Cu^{2+}, Fe^{3+} and Pb^{2+} may act as potential interferents when they have been at high concentrations in the sensing moiety. Interference of Fe^{3+} can be eliminated by masking fluoride at appropriate ionic strength and pH.

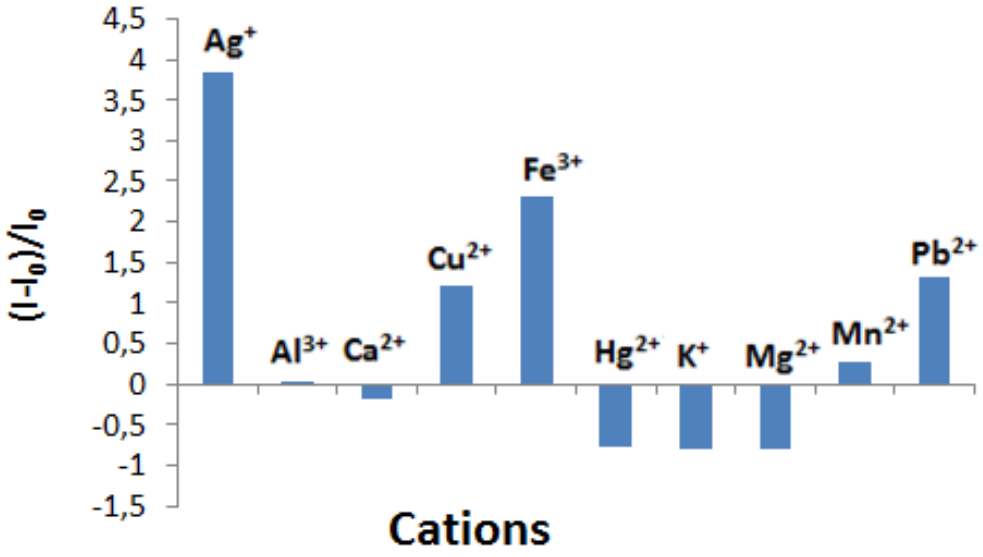

Figure 3.12 Metal ion response of EC based thin film at pH near natural pH in phosphate buffered solutions

Conventional anions of NO_3^-, NO_2^-, Cl^-, F^-, Br^-, SO_4^{2-}, PO_4^{3-}, were also tested. The observed response fort he listed anions was less than 5 %. As a conclusion, response of the Y10 dye is quite selective for Ag+ over most of the other convenient ions like Ca^{2+}, Mg^{2+}, K^+, and NO_3^-.

CHAPTER FOUR
CONCLUSION

Today, ionic or metallic forms of silver are intensively used in many different fields due to its anti bacterial effect. The intensive interest towards silver and use of soluble silver formulations causes a serious contamination in water and over exposure to silver compounds. However, the Environmental Protection Agency (EPA) bring some limitations for the allowed concentrations of Ag(I) which is lower than 1.6 nM for the aquatic life and less than 0.9 mM in drinking water (EPA, 1980).Therefore, correct and sensitive analysis of ionic silver is an important research topic.

Herein we performed spectral characterization of the Y10 dye both in solution and solid phases by UV-vis. absorption, excitation and emission spectroscopy. Solution phase studies were performed in THF, EtOH and DCM. We embedded the dye in PVC, PMMA and EC matrices for solid phase studies. Our preliminary metal-cation test results oriented as to study in the EC matrix. In later parts of the study we focused on EC-based tests. The Y10 dye exhibited both absorption and emission based response towards silver ions as low as 10^{-12} M when embedded in EC along with ionic liquid and other additives. Therefore, we prepared thin film and electrospun fibers of the Y10 dye for silver sensing purposes. The pH dependency of the dye has been investigated for the pH range of 2.0-7.0 and 7.0-12.0. The phosphate buffered solutions with a pH of 7.06 were chosen as the working pH

UV based response of the EC encaptulated Y10 dye has been investigated both for IL-free and IL-doped composites on thin films for a large concentration range of 10^{-12}- 10^{-5} M. Both forms of the dye exhibited a lineer absorption based response for the Ag^{+} ions. However, while the IL-Free composities exhibiting an increasing response in signal intensity the IL-Doped sensing agents yielded a decreasing absorption.

The excitation-emission based response of the Y10 dye was tested for pH and ionic silver for both thin film and electrospun fibers. In parallel to absorption based

results, the IL-Free and IL-Doped composities exhibited opposite signal change in direction when exposed to silver ions. The IL-doped composities exhibited larger working range with respect to the IL-Free forms. In case of thin films the working ranges of 10^{-12}-10^{-8} and 10^{-12}-10^{-4} M Ag^{+} were reported for the IL-Free and IL-Doped materials. The electrospun mats exhibited similar behavior to thin films and response range was reported as 10^{-12}-10^{-9} M and 10^{-12}-10^{-8} M for the IL-Free and IL-Doped sensing agents.

In addition to steady state mode measurements we also recorded the decay times of the different forms in the absence and presence of the ionic silver. However, the relative changes observed for the decay time measurements were not as high as the steady state mode. Therefore, we used the intensity based measurements for the calibration studies.

The Y10 dye, when encapsulated in EC along with IL, exhibited selective response towards Ag^{+} ions over Hg^{2+}, Al^{3+}, Ca^{2+}, Cu^{2+}, Fe^{3+}, K^{+}, Mn^{2+}, Mg^{2+}, Pb^{2+} ions in phosphate buffered solutions at pH 7.0.The excitation wavelength of 466 nm correspondes to blue LED region which allows miniaturization of the sensing design as a portable sensor when equiped with a diode and optical fibers.

REFERENCES

Aydogdu, S., Ertekin, K., Gocmenturk, M., Ergun, M., & Celık, E. (2014). Emission based sensing of subnanomolar dissolved carbon dioxide exploiting electrospun nanofibers. *International Journal of Polymeric Materials and Polymeric Biomaterials, 63*, 197–206.

Baldini F. et al. (eds.) (2006). Optical Chemical Sensors, 297–321, *Springer*. Printed in the Netherlands.

Borgohain, R., Boruah, P.K., & Baruah, S. (2016). Heavy-metal ion sensor using chitosan capped ZnS quantum dots. *Sensor and Actuators B: Chemical, 226,* 534-539.

Coskun, A., & Akkaya, E. U. (2005) Ion sensing coupled to resonance energy transfer: a highly selective and sensitive ratiometric fluorescent chemosensor for Ag (I) by a modular approach. *Journal of the American Chemical Society 127*, 10464–10465

Dey, S., Sarkar, S., Maity, D., & Roy, P. (2017). Rhodamine based chemosensor for trivalent cations: Synthesis, spectral properties, secondary complex as sensor for arsenate and molecular logic gates. *Sensor and Actuators B: Chemical, 246,* 518-534.

Englich, F.V., Foo, T.C., Richardson, A.C., Ependorff-Heidepriem, H., Sumby, C.J., & Monro, T.M. (2011). Photoinduced electron transfer based Ion sensing within an optical fiber. *Sensors, 11*, 9560-9572.

Ensafi, A. A., & Bakhshi, M., (2003). New stable optical film sensor based on immobilization of 2-amino-1-cyclopentene-1-dithiocarboxylic acid on acetyl cellulose membrane for Ni(II) determination . *Sensors and Actuators* B: *Chemical*, *96*, 435-440.

EPA (Environmental Protection Agency) (1980) *Ambient water quality criteria for silver*. EPA 4405–80-071. Office of Water Regulations, Washington DC

Ertekin, K., Tepe, M., Yenigül, B., Akkaya, E.U., & Henden, E. (2002). Fiber optic sodium and potassium sensing by using a newly synthesized squarine dye in PVC matrix. *Talanta, 58*, 719-727.

Fluorescence fundamentals, (2015). Retrieved June 5, 2015, from https://www.lifetechnologies.com/tr/en/home/references/molecular-probes-the-handbook/introduction-to-fluorescence-techniques.html#head1

Gong, T., Yang, W., Zhang, M., Zhou, W., & Xue, R. (2018). Reversible ratiometric silver ion and pH probe constructed from a quinoline-containing diphenylsulfone derivative with AIEE effect. *Journal of Material Science*, *53*, 13900-13911.

He, X.P., Song, Z., Wang, Z.Z., Shi, X.X., Chen, K., & Chen, G.R. (2011) Creation of 3,4-bis-triazolocoumarinesugar conjugates via flourogenic dual click chemistry and their quenching specificity with silver(I) in aqueous media. *Tetrahedron 67,* 3343-3347

IUPAC (International Union of Pure Applied Chemistry) (1996). *Glossary of terms used in photochemistry, 68*, 2248.

Iyoshi, S., Taki, M., & Yamamoto, Y. (2008) Rosamine-based fluorescent chemosensor for selective detection of silver (I) in an aqueous solution. *Inorganic Chemical 47*, 3946–3948

Jerónimo, P.C.A., Araújo, A.N., & Montenegro, M.C.B.S.M. (2007). Optical sensors and biosensors based on sol-gel films. *Talanta,72*, 13-27.

Kaçmaz, S., Ertekin, K., Suslu A., Ozdemir, M., Ergun, Y., Celik, E., Cocen, U. (2011). Emission based sub-nanomolar silver sensing with electrospun nanofibers. *Sensors and Actuators B: Chemical, 153*, 205-213.

Kandaz, M., Güney O., & Senkal, F. B. (2009) Fluorescent chemosensor for Ag (I) based on amplified fluorescence quenching of a new phthalocyanine bearing derivative of benzofuran. *Polyhedron 28,* 3110–3114

Kang, J. H., Chae, J. B., & Kim, C. (2018). A multi-functional chemosensor for highly selective ratiometric fluorescent detection of silver (I) ion and dual turn-on fluorescent and colorimetric detection of sulfide. *Royal Society Open Science*, *5*, 180293.

Kermis, R.H., Kostov, Y., & Rao, G. (2003). Rapid method for the preparation of a robust optical pH sensor. *Analyst 128*, 1181-1186.

Lakowicz, J. R. (1993). *Principles of fluorescence spectroscopy.* Plenum Press: New York and London.

Langhals, H., Ismael, R., & Yuruk, O. (2000) Persistent fluorescence of perylene dyes by steric inhibition of aggregation. *Tetrahedron 56,* 5435–5441

Lang, M., Li, Q., Huang, H., Yu, F., & Chen, Q. (2016) Highly sensitive exonuclease III-assisted fluorometric determination of silver(I) based on graphene oxide and self-hybridization of cytosine-rich ss-DNA. *Microchimica Acta 183,* 1659–1665

Liao, S., Zhao, X., Zhu, F., Chen, M., Wu, Z., Song, X., Yang, H., & Chen, X. (2018). Novel S, N-doped carbon quantum dot-based “off-on” fluorescent sensor for silver ion and cysteine. *Talanta 180*, 300-308.

Liu, M., Xu, Z., Song, Y., Li, H., Xian, C. (2018). A novel coumarin-based chemosensor for colorimetric detection of Ag(I) ion and fluorogenic sensing of Ce(III) ion. *Journal of Luminescence, 198*, 337-341.

Lukowiak, A., & Strek, W., (2009). Sensing abilities of materials prepared by sol-gel technology. *J Sol-gel Sci Technol, 50,* 201-215.

Lobnik, A., Oehme, I., Murkovic, I., & Wolfbeis, O.S. (1998) pH optical sensors based on sol-gels: Chemical doping versus covalent immobilization. *Analytica Chimica Acta 367*, 159-165.

Lobnik, A., Turel M., & Urek, Š. K. (2012). *Optical chemical sensors: Design and applications*. Retrieved October 05, 2012, from http://www.intechopen.com/books/advances-in-chemical-sensors/opticalchemical-sensors-design-and-applications

Lotfi, B., Tarlani, A., Akbari-Moghaddam, P., Mirza-Aghayan, M., Peyghan, A. A., Muzart, J., & Zadmard, R. (2017). Multivalent calix[4]arene-based fluorescent sensor for detecting silver ions in aqueous media and physiological environment. *Biosensors and Bioelectronics 90*, 290-297.

McDonagh, C., Burke, C.S., & MacCraith, B.D. (2008). Optical Chemical Sensor. *Chemical Reviews,108,* (2), 400-422.

Mayr, T. (2002). *Optical sensors for the determination of heavy metals*. Retrieved November 26, 2012.

Mohr, G. J. (2002). *Materials and polymers in optical sensing.* Retrieved November 08, 2012, from http://www2.uni-jena.de/~c1moge/Mohr/ASCOS2002.pdf

Nugent, J.W., Lee, H., Reibenspies, J.H., Lee, H.S., & Hancock, R.D. (2017). Effects of anion coordination on the fluorescence of a photo-induced electron transfer (PET) sensor complexed with metal ions. *Polyhedron, 130*, 47-57.

Oehme, I., & Wolfbeis, O.S. (1997). Fundamental Review: Optical Sensors for Determination of Heavy Metal Ions. *Mikrochim. Acta, 126*, 177-192.

Ongun, M. Z., Ertekin, K., Gocmenturk, M., Ergun, Y., & Suslu, A. (2012). Copper ion sensing with fluorescent electrospun nanofibers. *Spectrochim Acta A Mol Biomol Spectrosc. 90*, 177-185.

Ongun, Zeyrek, M., Ertekin, K., Nadeem, S., & Birel, O. (2016). Polyoxy-derivatized perylenediimide as Selective Fluorescent Ag (I) Chemosensor. *Journal of Fluorescence, 26*, 2311-2320.

Oter, O. *(2007). Investigation of Sensor Characteristics of Some Chromoionophore Structures in Polymer and Sol-Gel Matrices.* Ph.D Thesis. Dokuz Eylül University, Izmir.

Parker, C. (1968). *Photoluminescence of solutions (1 st ed.).* Amsterdam: Elsevier. Schmidt, W. (1994). *Optische Spectroskopie*. VCH: Weinheim.

Paul, A., Mandal, P. K., & Samanta, A. (2005) On the optical properties of the imidazolium ionic liquids. *Journal of Physical Chemistry B, 109*(18), 9148-9153.

Saleh, S.M., Elkady, E.M., Ali, R., Alminderej, F., & Mohamed, T.A. (2018). Novel chemical sensor for detection Ca(II) ions based on ferutinin. *Spectrochimica Acta Part A: Molecular and Biomolecular Spectroscopy, 205*, 264-268.

Schulman, G.S., Chen, S., Bai, F., Leiner, MJP., Weis, L., & Wolfbeis, O.S. (1995). Dependence of the fluorescence of immobilized 1-hydroxypyrene-3,6-trisulfonate on solution pH: extension of the range of applicability of a pH fluorosensor. *Analytica Chimica Acta 304*,165-170.

Shamsipur, M., Alizadeh, K., Hosseini, M., Caltagirone, C., & Lippolis, V. (2006) A selective optode membrane for silver ion based on fluorescence quenching of the dansylamidopropyl pendant arm derivative of 1-aza-4,7,10-trithiacyclododecane([12]aneNS3*). Sensor and Actuators B 113*, 892–899

Sinha, N., Jain, S., Tilekar, A., Upadhayaya, R. S., Kishore, N., Jana G. H. & Arora, S. K. (2005). Synthesis and antimycobacterial evaluation of nitroheterocyclic-based 1, 2, 4 -benzothiadiazines. *Bioorganic & Medicinal Chemistry Leetrs, 15*(6), 1573-1576.

Stetter, J. R., Penrose, W. R., & Yao, S. (2003). Sensors, chemical sensors, electrochemical sensors, and ECS. *Journal of the Electrochemical Society, 150* (2), 11-16.

Su, P., Zhu, Z., Wang, J., Cheng, B., Wu, W., Iqbal, K., Tang, Y. (2018). A biomolecule-based fluorescence chemosensor for sequential detection of Ag^{+} and H_2S in 100% aqueous solution and living cells. *Sensors and Actuators B: Chemical*, 273, 93-100.

Sun, H., Lai, J. P., Lin, D. S., Huang, X. X., Zuo, Y., & Lia, Y. L. (2016) A novel fluorescent multi-functional monomer for preparationof silver ionimprinted fluorescent on–off chemosensor. *Sensors and Actuators B Chemical 224*, 485–491

Tian, Y., Fuller, E., Klug, S., Lee, F., Su, F., Zhang, L., Chao, S., & Meldrum, D. (2013) A fluorescent colorimetric pH sensor and the influences of matrices on sensing performances. *Sensors and Actuators* B *188*, 1-10.

Topal, S.Z., Gürek, A.G., Ertekin, K., Atilla, D., Yenigül, B., & Ahsen, V. (2010). Silver and proton driven fluorescent multiple-mode molecular logic gates employing phthalocyanines. *Materials Chemistry and Physics, 121*, 425-431.

Topal, S.Z., Gürek, A.G., Ertekin, K., Yenigul, B., & Ahsen, V. (2010) Fluorescent probes for silver detection employing phthalocyanines in polymer matrices. *Sensor Letters 8*, 1–8

Uyar, T., Balan, A., Toppare, L., & Redenbacher, F. (2009). Electrospinning of cyclodextrin functionalized poly(methyl methacrylate) (PMMA) nanofibers. *Polymer*, *50*(2) 475-480.

Veale, E. B., & Gunnlaugsson, T. (2010). Fluorescent sensors for ions based on organic structures. *Annual Reports. Program. Chemical Sect. B, 106*, 376–406.

Valeur, B., & Berberan-Santos, M. N. (2002). *Molecular fluorescence: Principles and applications.* John Wiley & Sons.

Venturini, F., Baumgartner, M., & Borisov, S.M. (2018). Mn^{4+}-doped magnesium titanate—a promising phosphor for self-referenced optical temperature sensing. *Sensors, 18*, 668.

Weidgans, B.M., Krause, C., Klimant, I., & Wolfbeis, O.S. (2004) Fluorescent pH sensors with negligible sensitivity to ionic strength. *Analyst 129*, 645–650.

Wencel, D., Abel, T., & McDonagh, C. (2014). Optical Chemical pH Sensors. *Analytical Chemistry*, *86*, 15-29.

Wang, H., Xue, L., Qian, Y., & Jiang, H. (2010) Novel ratiometric fluorescent sensor for silver ions. *Organic Letters 12*, 292–295

Wang, H. H., Xue, L., Qian, Y. Y., & Jiang, H. (2010) Novel ratiometric fluorescent sensor for silver ions. *Organic Letters 12*(2), 292-295.

Wei, T., Zhang, H., Li, W., Qu, W., Su, J., Lin, Qi., Zhang, Y., & Yao, H. (2017). Sensitive and selective fluorescent and colorimetric sensor for Ag^{+} based on the supramolecular self-assembly in semi-water. *Chinese Journal of Chemistry, 35,* 1311-1316.

Yanar, U., Babür, B., Pekyılmaz, D., Yahaya, I., Aydıner, B., Dede, Y., & Seferoğlu, Z. (2016). A fluorescent coumarin-thiophene hybrid as a ratiometric chemosensor for anions: Synthesis, photophysics, anion sensing and orbital interactions. *Journal of Molecular Structure, 1108,* 269-277.

Zeyrek Ongun, M. (2013). *Development of Nano Material Based Sensors for Determination of Some-Cation/Anion in Groundwater and Complementary Usage of Ion Chromatography.* Ph.D Thesis. Dokuz Eylül University, Izmir.

Zeyrek, M. (2008*). Determination of anions in geothermal waters with ion chromatography and bicarbonate with spectroscopic method*. M. Sc Thesis. Dokuz Eylül University, Izmir.

Zhang, Y., Chen, X., Liang, G., Zhong, K., Lin, Q., Yao, H., & Wei, T. (2018). A novel water soluble pillar[5]arene and phenazine derivative self-assembled pseudorotaxane sensor for the selective detection of Hg^{2+} and Ag^{+} with high selectivity and sensitivity. *New Journal of Chemistry, 42,* 10148.

Zhao, X., Lei, C., Gao, Y., Zhu, S., Yang, X., You, J., & Wang, H. (2017). A ratiometric fluorescent nanosensor for the detection of silver ions using graphene quantum dots. *Sensor and Actuators B: Chemical, 253,* 239-246.

Zhu, B., Xu, M., Qian, C., Han, L., Gao, J., Ye, Q., & Li, Y. (2018). Synthesis and fluorescence characteristics of selective ratiometric fluorescent sensors for silver

ions based on 3-indolyl-4-indazolyl maleimide derivatives. *Research on Chemical Intermediates, 44*, 3985-3999.